Modeling Stability and Control of Tokamaks with Resistive Walls

D.P. Brennan[1], A.J. Cole[2], J.M. Finn[3], M.R. Halfmoon[4], D.J. Rhodes[2]

[1]Princeton Plasma Physics Laboratory
[2]Columbia University
[3]Los Alamos National Laboratory
[4]University of Tulsa

Research Review Seminar Series
PPPL
April 22, 2016

Princeton University · Columbia University in the City of New York · Los Alamos National Laboratory EST. 1943 · The University of Tulsa

Collaborative team effort combines extended MHD computation with reduced modeling to address puzzles

Motivation: Several computational and experimental puzzles involving extended MHD instabilities drive the need for reduced modeling to gain understanding

Computational tools for experimental analysis (in this talk):

- NIMROD: Nonlinear toroidal extended MHD with δf kinetic PIC
- PEST-III: Linear toroidal resistive MHD

Reduced resistive MHD model of cylindrical tokamak serves as basis: modular additions depending on problem:

- toroidal field line curvature to couple modes in a cylindrical model
- trapped energetic ions
- differential flow between surfaces and/or a wall
- a resistive wall
- feedback control from external coils

OUTLINE

Review the simple reduced MHD model with

- differential flow between surfaces and/or a wall
- a resistive wall
- feedback control from external coils
- toroidal field line curvature in a cylindrical model
- trapped energetic ions

Brief Review: 2016 Sherwood Theory Conference presentations

J.M. Finn	Toroidal mode coupling model derivation Double tearing vs. Toroidal coupling via pressure
D.J. Rhodes	Beta ordering can change due to qmin or toroidal curvature, coupling Shaping effects important
D.P. Brennan	Toroidal coupling model explanation of 2/1 onset and rotation effect
M.R. Halfmoon	Energetic particle effects on resistive and ideal MHD modes explains effect of core shear
A.J. Cole	Locking to the backward propogating wave finite frequency modes drive flow at surface

OUTLINE

Review the simple reduced MHD model with

- differential flow between surfaces and/or a wall
- a resistive wall
- feedback control from external coils
- toroidal field line curvature in a cylindrical model
- trapped energetic ions

Brief Review: 2016 Sherwood Theory Conference presentations

J.M. Finn	Toroidal mode coupling model derivation Double tearing vs. Toroidal coupling via pressure
D.J. Rhodes	Beta ordering can change due to qmin or toroidal curvature, coupling Shaping effects important
D.P. Brennan	Toroidal coupling model explanation of 2/1 onset and rotation effect
M.R. Halfmoon	Energetic particle effects on resistive and ideal MHD modes explains effect of core shear
A.J. Cole	Locking to the backward propogating wave finite frequency modes drive flow at surface

Stability analysis with flow and proportional gain

Basis function method (from early Culham years?)

Example for one surface and one resistive wall with control coil : separate solution into zones with superimposed solution components shielded from neighboring resonant surfaces or conducting walls.

Further separate solution into plasma response (ψ_1) and the resistive wall/control coil external solution (ψ_2)

Simplifies the analysis into 2x2 matrix for ψ_1 and ψ_2. ψ_3 then determined.

Similar approach taken for several different models.

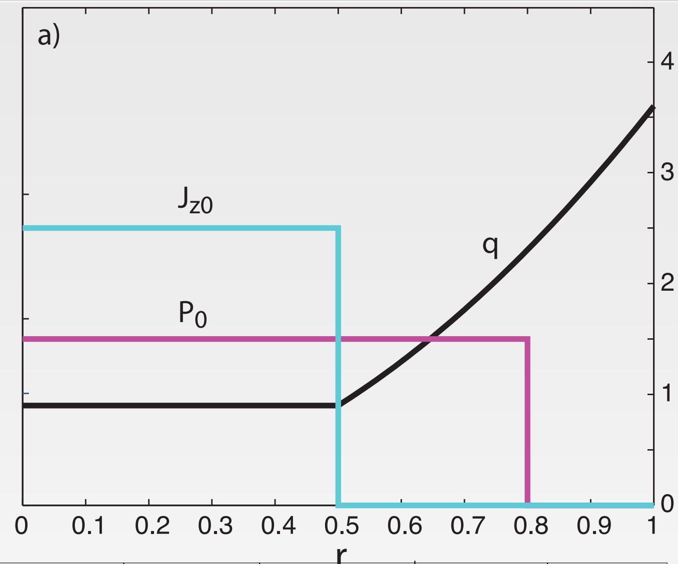

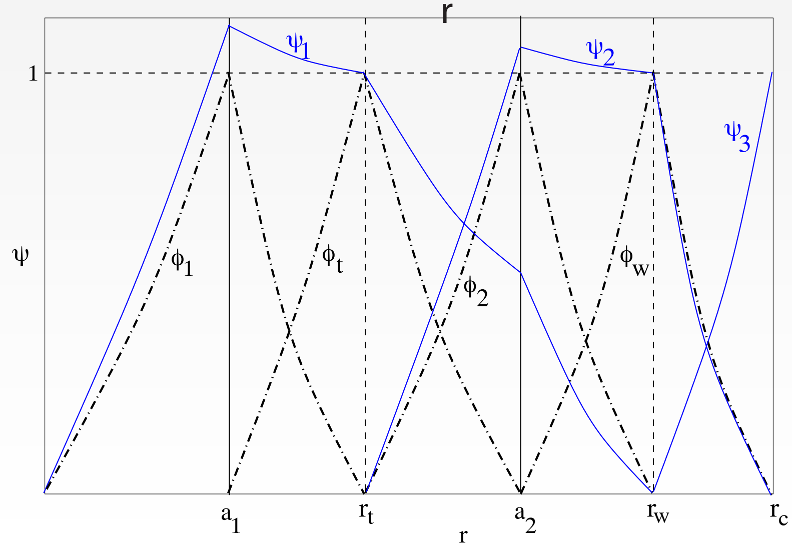

Stability analysis with flow and proportional gain

Three conditions for three unknowns in the "Culham" method:

$$\tilde{\psi}(r) = \alpha_1\psi_1(r) + \alpha_2\psi_2(r) + \alpha_3\psi_3(r)$$

Resonant surface

$$\gamma_d \tau_t \psi(r_t) = \left[\psi'\right]_{r_t}$$

Resistive wall

$$\gamma \tau_w \psi(r_w) = \left[\psi'\right]_{r_w}$$

Describes the resistive plasma resistive wall mode

$$\begin{pmatrix} \Delta_1 - \gamma\tau_t & l_{21} \\ l_{12} & \Delta_2 - \gamma\tau_w \end{pmatrix}\begin{pmatrix} \alpha_1 \\ \alpha_2 \end{pmatrix} = 0$$

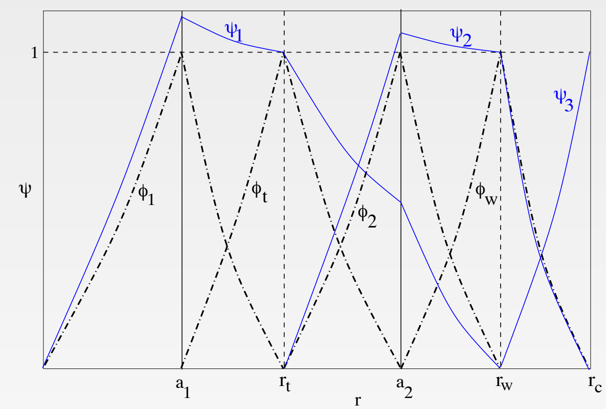

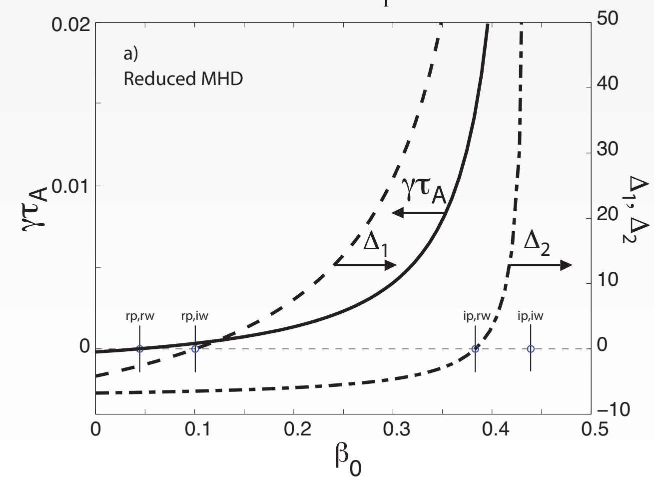

Stability can be understood in terms of four β limits, with and without resistivity in wall and plasma

$\beta_{rw,rp}$ Is the lowest/first boundary

$\beta_{iw,rp}$ and $\beta_{rw,ip}$ can in principle change order, here $\beta_{iw,rp} < \beta_{rw,ip}$

$\beta_{iw,ip}$ is the highest boundary

Physics of stability windows with control can be understood in terms of these limits

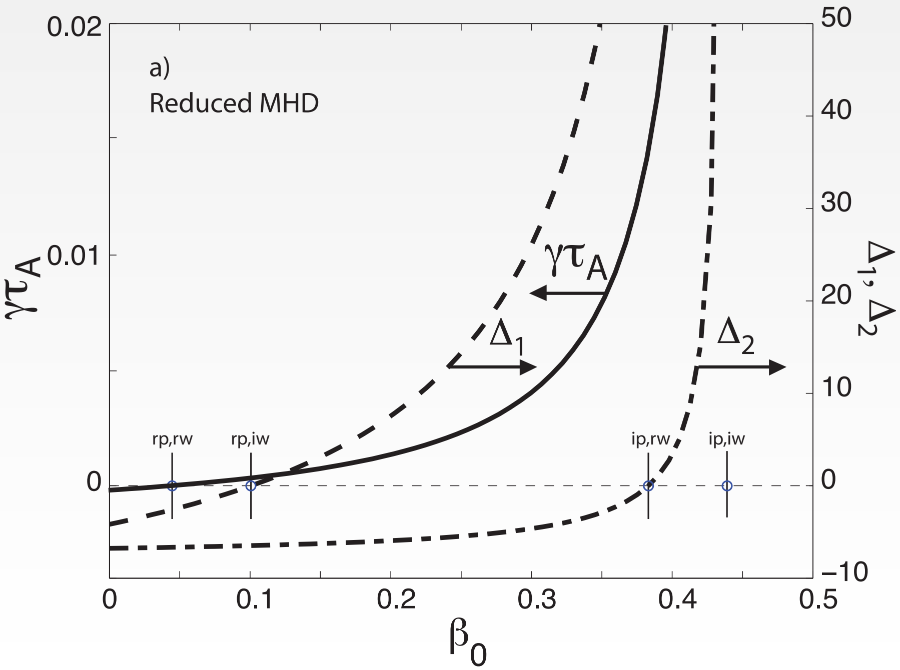

Stability analysis with flow and proportional gain

Three conditions for three unknowns in the "Culham" method:

$$\tilde{\psi}(r) = \alpha_1 \psi_1(r) + \alpha_2 \psi_2(r) + \alpha_3 \psi_3(r)$$

Resonant surface

$$\gamma_d \tau_t \psi(r_t) = [\psi']_{r_t} \qquad \gamma_d \equiv \gamma + i\Omega$$

Resistive wall

$$\gamma \tau_w \psi(r_w) = [\psi']_{r_w}$$

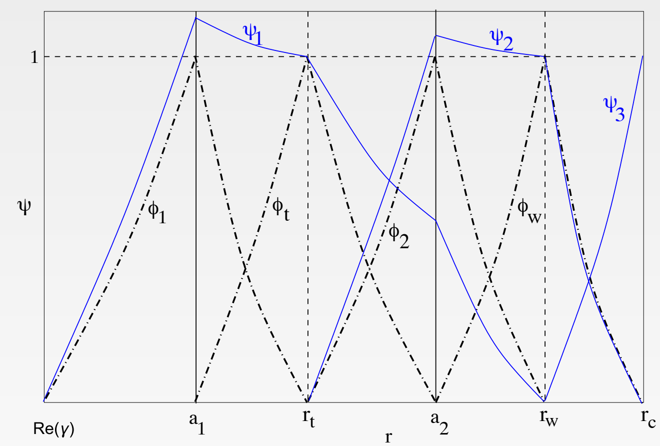

Including rotation at the surface can be approximated simply by a Doppler shift of the layer response.

$$\begin{pmatrix} \Delta_1 - (\gamma + i\Omega)\tau_t & l_{21} \\ l_{12} & \Delta_2 - \gamma\tau_w \end{pmatrix} \begin{pmatrix} \alpha_1 \\ \alpha_2 \end{pmatrix} = 0$$

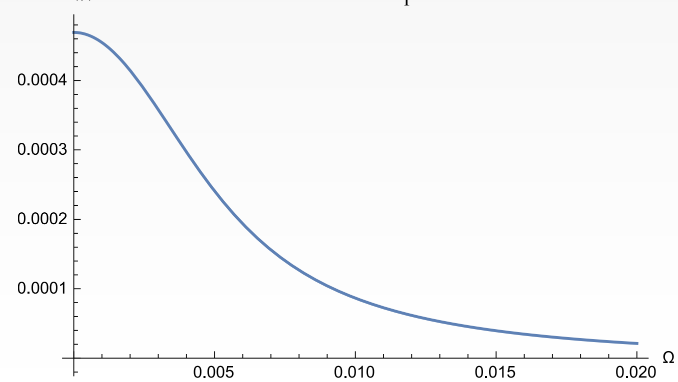

Two Sensor Feedback Control Equation

- **Feedback boundary condition at r_c is proportional gain applied a linear combination of components of the fluctuation measured at the wall:**

$$\tilde{B}_r(r_c) = -(r_w/r_c)\{G\tilde{B}_r(r_w) + iK[\mathbf{k}\cdot\tilde{\mathbf{B}}(r_w^-)]\}$$

$$\mathbf{k} \equiv (m/r)\hat{\theta} + k\hat{z}$$

$$\boldsymbol{\sigma} \equiv \hat{r}\times\mathbf{k} = (m/r)\hat{z} - k\hat{\theta}$$

Tangential measurement is more effective inside

The effect of two walls reported in RFP study: Sassenberg PPCF 2013.

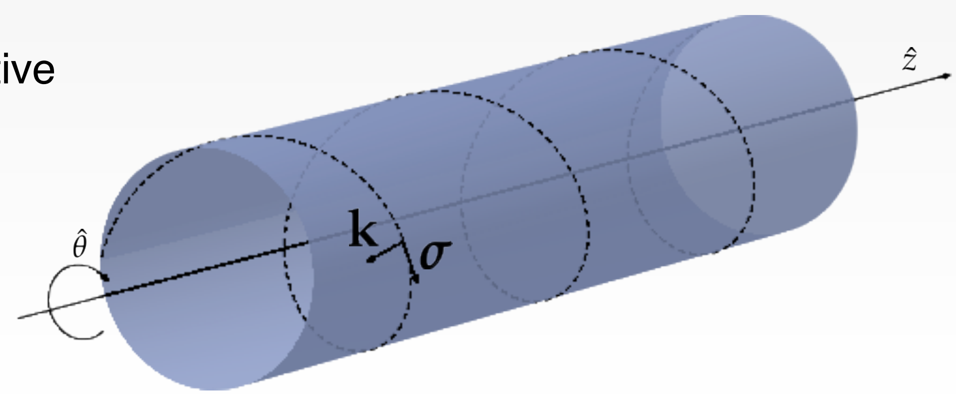

Stability analysis with flow and proportional gain

Three conditions for three unknowns in the "Culham" method:

$$\tilde{\psi}(r) = \alpha_1\psi_1(r) + \alpha_2\psi_2(r) + \alpha_3\psi_3(r)$$

Resonant surface

$$\gamma_d \tau_t \psi(r_t) = [\psi']_{r_t} \qquad \gamma_d \equiv \gamma + i\Omega$$

Resistive wall

$$\gamma \tau_w \psi(r_w) = [\psi']_{r_w}$$

Control Coil

$$\psi(r_c) = -G\psi(r_w) + K\psi'(r_{w-})$$

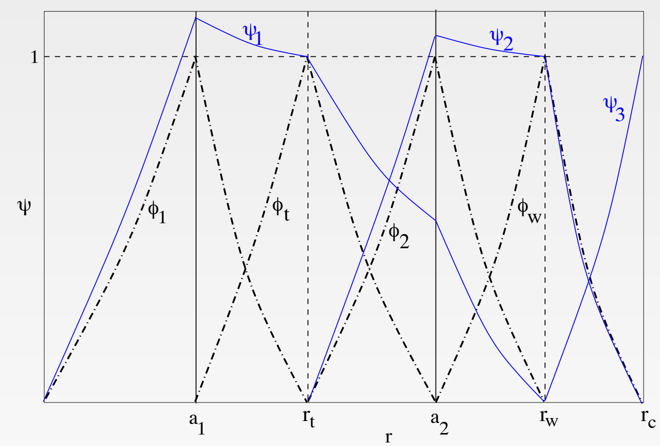

Adding in control coils with complex gain allows

$$\begin{pmatrix} \Delta_1 - (\gamma + i\Omega)\tau_t & l_{21} \\ l_{12} - Kl_{32}l_{12} & \Delta_2 - Gl_{32} + Kl_{32}l_{22}^{(-)} - \gamma\tau_w \end{pmatrix} \begin{pmatrix} \alpha_1 \\ \alpha_2 \end{pmatrix} = 0$$

Complex Gain in G effectively the same as a rotating wall
Finn Chacon PPCF 04
Complex K less intuitive

D.P. Brennan and J.M. Finn, Phys. Plasmas 21, 102507 (2014).

Stability analysis with flow and proportional gain

Crossing $\beta_{rp,iw}$ when left boundary vertical

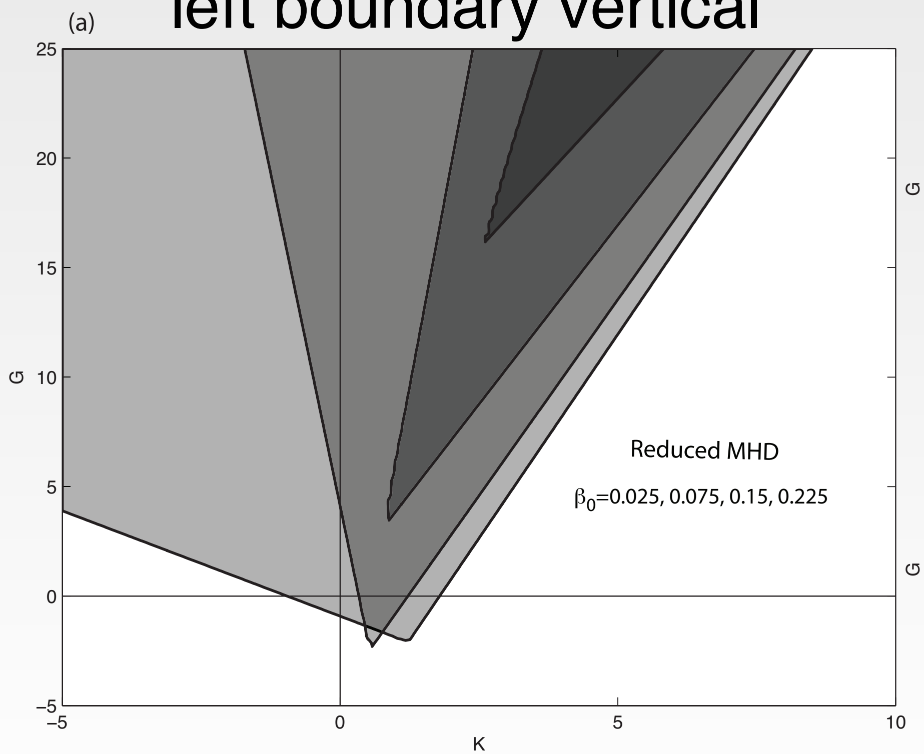

Effect of Ω stabilizing below $\beta_{rp,iw}$ (destabilizing above)

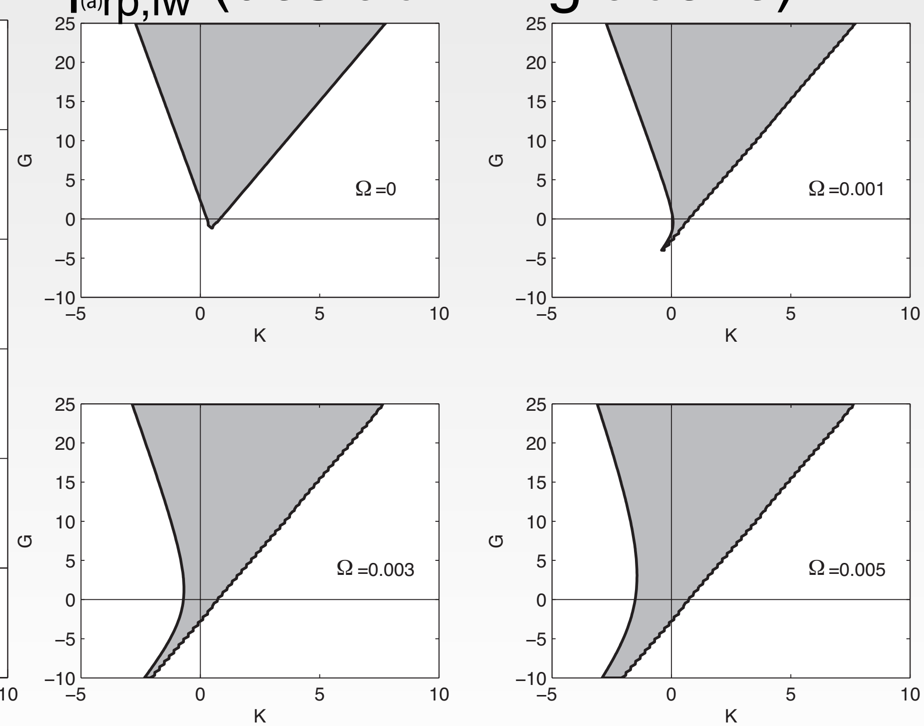

Several findings associated with optimal gains on radial and tangential sensors, and complex responses

D.P. Brennan and J.M. Finn, Phys. Plasmas 21, 102507 (2014).

OUTLINE

Review the simple reduced MHD model with

- differential flow between surfaces and/or a wall
- a resistive wall
- feedback control from external coils
- toroidal field line curvature in a cylindrical model
- trapped energetic ions

Brief Review: 2016 Sherwood Theory Conference presentations

J.M. Finn	Toroidal mode coupling model derivation Double tearing vs. Toroidal coupling via pressure
D.J. Rhodes	Beta ordering can change due to qmin or toroidal curvature, coupling Shaping effects important
D.P. Brennan	Toroidal coupling model explanation of 2/1 onset and rotation effect
M.R. Halfmoon	Energetic particle effects on resistive and ideal MHD modes explains effect of core shear
A.J. Cole	Locking to the backward propogating wave finite frequency modes drive flow at surface

A Reduced Model for Coupled Modes in Flow

Using an analysis similar to Brennan Finn, PoP 14 specify a step function equilibrium

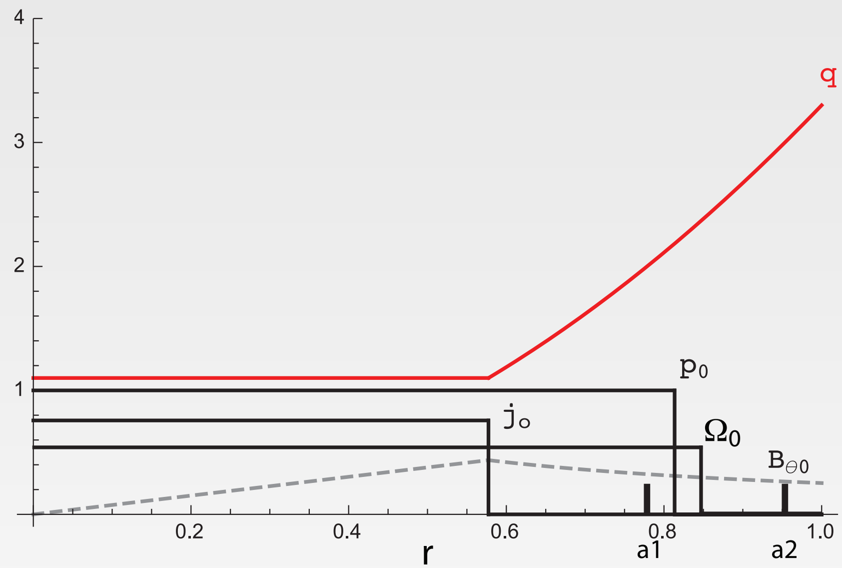

q is specified to have two rational surfaces with m_1=2 and m_2=m_1+1=3.
Rotation Ω is included only in the layer at m_1

Inner surface has flow Ω_0
while outer surface no flow -> Doppler shift $\gamma \rightarrow \gamma + i\Omega_0$ for inner surface only.

Separate, overlapping mode components couple through pressure

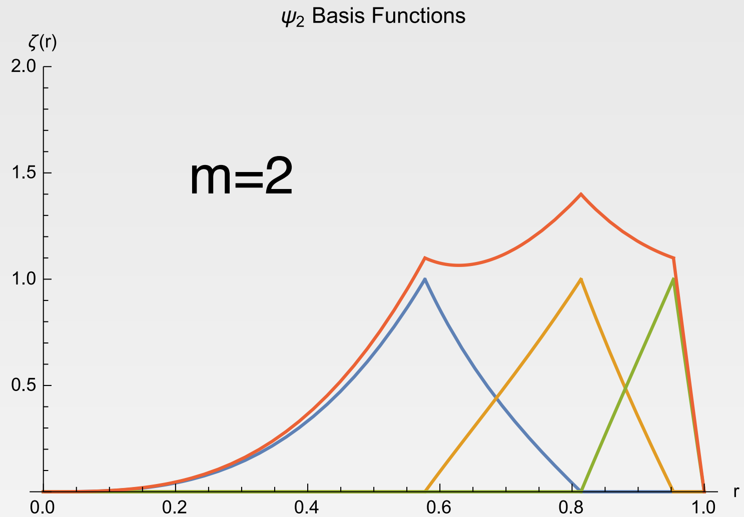

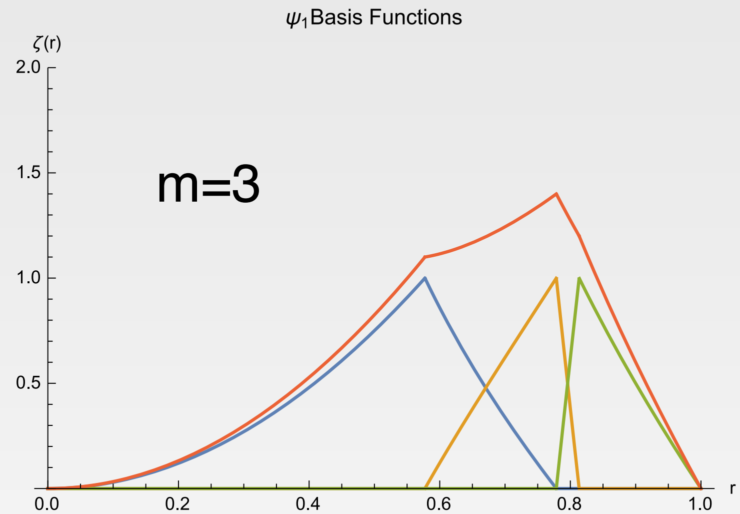

We solve the outer region equations for two overlapping perturbations with m_1 and m_2 coupled through the pressure at a_p:

$$\tilde{\psi}(r,\theta,\varphi) = (\alpha_1 \psi_1(r) e^{im_1\theta} + \alpha_2 \psi_2(r) e^{im_2\theta}) e^{-in\varphi}$$

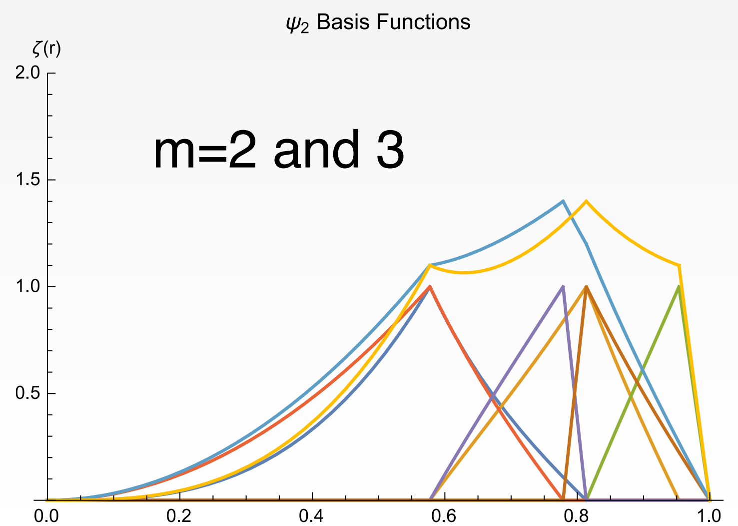

The basis sets reflect that each is independently resonant at their own surface, but both respond to current and pressure steps -> coupling.

The perturbations couple through the toroidal curvature

Including toroidicity in field line curvature we can write

$$\kappa \cdot \hat{r} = \kappa(\theta) = \kappa_0 + \kappa_1 \cos(\theta)$$

Where the flux averaged part of the curvature becomes

$$\kappa_0 = \left\langle \kappa_\varphi \cdot \hat{r} + \kappa_\theta \cdot \hat{r} \right\rangle = \frac{r}{2R_0^2} - \frac{B_\theta^2(r)}{rB_0^2} = -\frac{r}{R_0^2 q^2}(1-q^2)$$

Assume the poloidal curvature doesn't vary with θ, then the poloidally varying part, which will couple the m's, comes only from the toroidal curvature

$$\kappa_1 = \kappa_t \cdot \hat{r} = -\frac{\cos(\theta)}{R_0} + \frac{r\cos(2\theta)}{2R_0^2} \approx -\frac{\cos(\theta)}{R_0}$$

The ideal outer region equation becomes:

$$B \cdot \nabla \nabla_\perp^2 \tilde{\psi} - \frac{2}{r}(\kappa_0 + \kappa_1 \cos\theta)\frac{\partial \tilde{p}}{\partial \theta} = 0$$

Note, for

$$\kappa_0 = -\frac{r}{R_0^2 q^2}, \ \kappa_1 = 0$$

We recover the cylinder and uncoupled modes

A Reduced Model for Coupled Modes in Flow

Substituting in

$$F_1(r)\alpha_1(\psi_1'' + \psi_1'/r - m_1^2\psi_1/r^2)e^{im_1\theta} + F_2(r)\alpha_2(\psi_2'' + \psi_2'/r - m_2^2\psi_2/r^2)e^{im_2\theta} +$$

$$\frac{2}{r}(\kappa_0 + \kappa_1\cos\theta)\left[\frac{m_1^2 p'(r)}{rF_1(r)}\right]\alpha_1\psi_1(r)e^{im_1\theta} + \frac{2}{r}(\kappa_0 + \kappa_1\cos\theta)\left[\frac{m_2^2 p'(r)}{rF_2(r)}\right]\alpha_2\psi_2(r)e^{im_2\theta} = 0$$

Separating out the θ dependencies, and integrating over the pressure step we find two coupled equations

$$\alpha_1[\psi_1']_{ap} - \alpha_1\psi_1(a_p)\frac{2m_1^2\kappa_0 p_0}{a_p^2 F_1^2(a_p)} - \alpha_2\psi_2(a_p)\frac{2m_2^2\kappa_1 p_0}{a_p^2 F_1(a_p)F_2(a_p)} = 0,$$

$$\alpha_2[\psi_2']_{ap} - \alpha_2\psi_2(a_p)\frac{2m_2^2\kappa_0 p_0}{a_p^2 F_2^2(a_p)} - \alpha_1\psi_1(a_p)\frac{2m_1^2\kappa_1 p_0}{a_p^2 F_1(a_p)F_2(a_p)} = 0$$

A Reduced Model for Coupled Modes in Flow

Reducing these to matrix form we can connect with standard cylindrical theory

$$\begin{bmatrix} ((\gamma + i\Omega_0)\tau_1 - \Delta_1)\left(\dfrac{\Delta_p - \Pi_{11}}{l_{p1}}\right) + l_{1p} & -(\gamma\tau_2 - \Delta_2)\left(\dfrac{\Pi_{12}}{l_{q2}}\right) \\ -((\gamma + i\Omega_0)\tau_1 - \Delta_1)\left(\dfrac{\Pi_{21}}{l_{p1}}\right) & (\gamma\tau_2 - \Delta_2)\left(\dfrac{\Delta_q - \Pi_{22}}{l_{q2}}\right) + l_{2q} \end{bmatrix} \begin{bmatrix} \alpha_1 \\ \alpha_2 \end{bmatrix} = 0$$

Where for zero coupling

$$(\gamma\tau_1 - \Delta)\left(\frac{\Delta_p - \Pi_{11}}{l_{p1}}\right) + l_{1p} = 0 \qquad (\gamma\tau_2 - \Delta_2)\left(\frac{\Delta_q - \Pi_{22}}{l_{q2}}\right) + l_{2q} = 0$$

Implemented in a few applications

OUTLINE

Review the simple reduced MHD model with

- differential flow between surfaces and/or a wall
- a resistive wall
- feedback control from external coils
- toroidal field line curvature in a cylindrical model
- trapped energetic ions

Brief Review: 2016 Sherwood Theory Conference presentations

J.M. Finn	Toroidal mode coupling model derivation Double tearing vs. Toroidal coupling via pressure
D.J. Rhodes	Beta ordering can change due to qmin or toroidal curvature, coupling Shaping effects important
D.P. Brennan	Toroidal coupling model explanation of 2/1 onset and rotation effect
M.R. Halfmoon	Energetic particle effects on resistive and ideal MHD modes explains effect of core shear
A.J. Cole	Locking to the backward propogating wave finite frequency modes drive flow at surface

Beta Ordering Altered by Toroidal Curvature Variation

Varying κ_1 can switch the two middle beta limits:

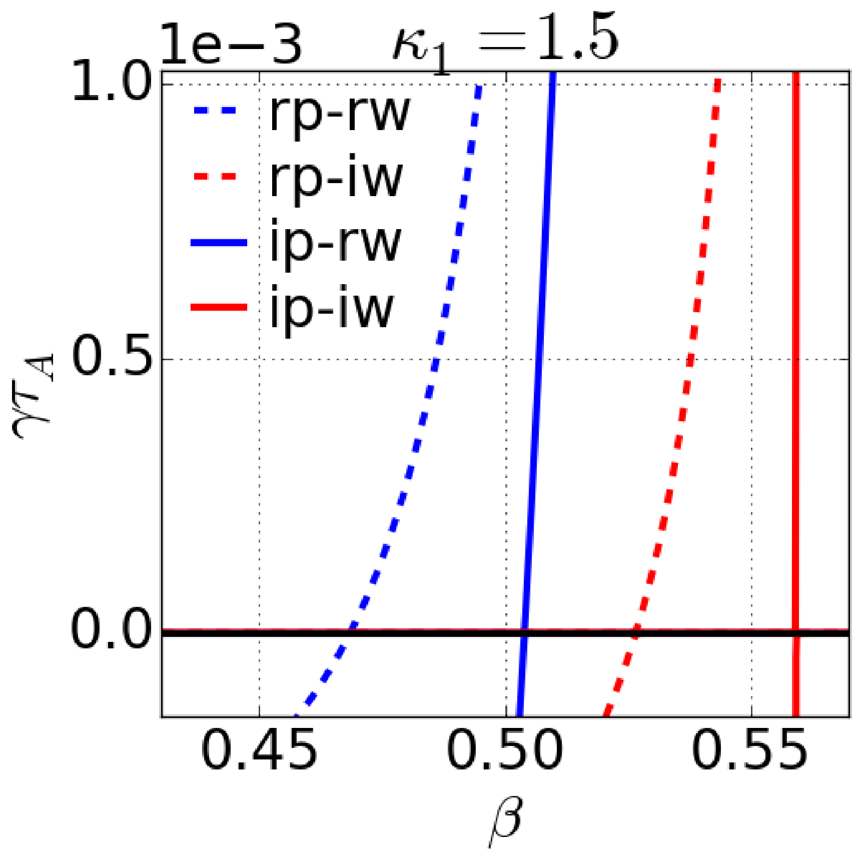

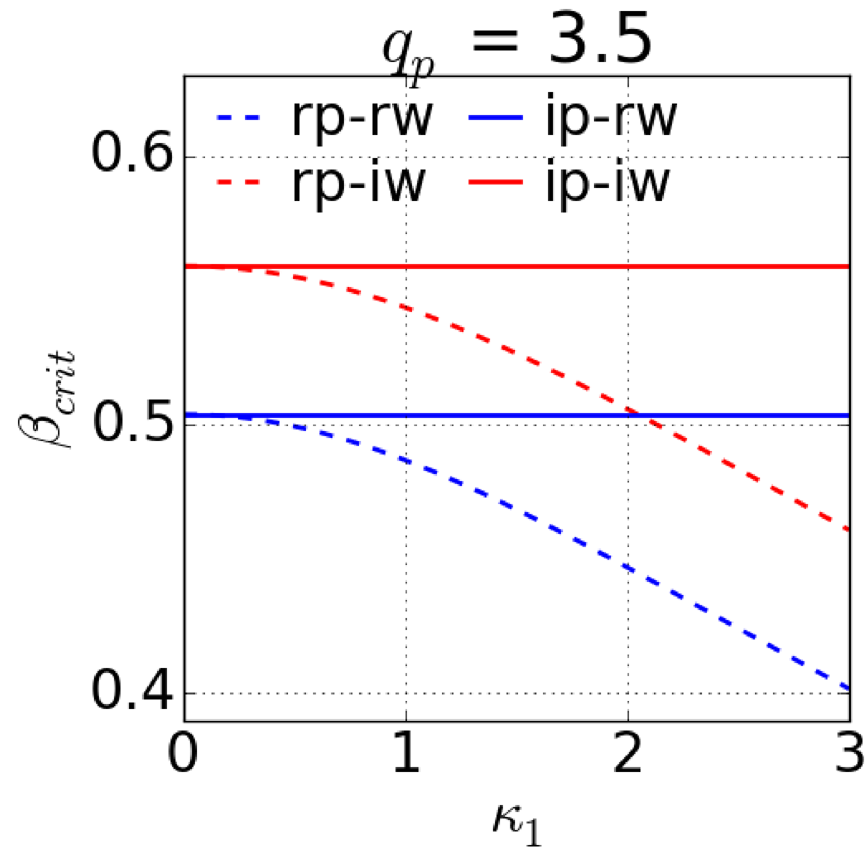

The cylindrical limit $\kappa \to 0$ reduces to two ideal modes.

$\Rightarrow$ **Tearing response driven purely by toroidal curvature.**

Beta Ordering Domains

The beta ordering domains for the two-tearing model are calculated analytically in $\kappa_1 - q_p$ space.

$$\beta_{rp-iw} = \frac{(\beta_1+\beta_2) - \sqrt{(\beta_1+\beta_2)^2 - 4\beta_1\beta_2\left[1-(\kappa_1/2)^2\right]}}{2\left[1-(\kappa_1/2)^2\right]} = \tilde{\beta}_1 = \beta_{ip-rw}$$

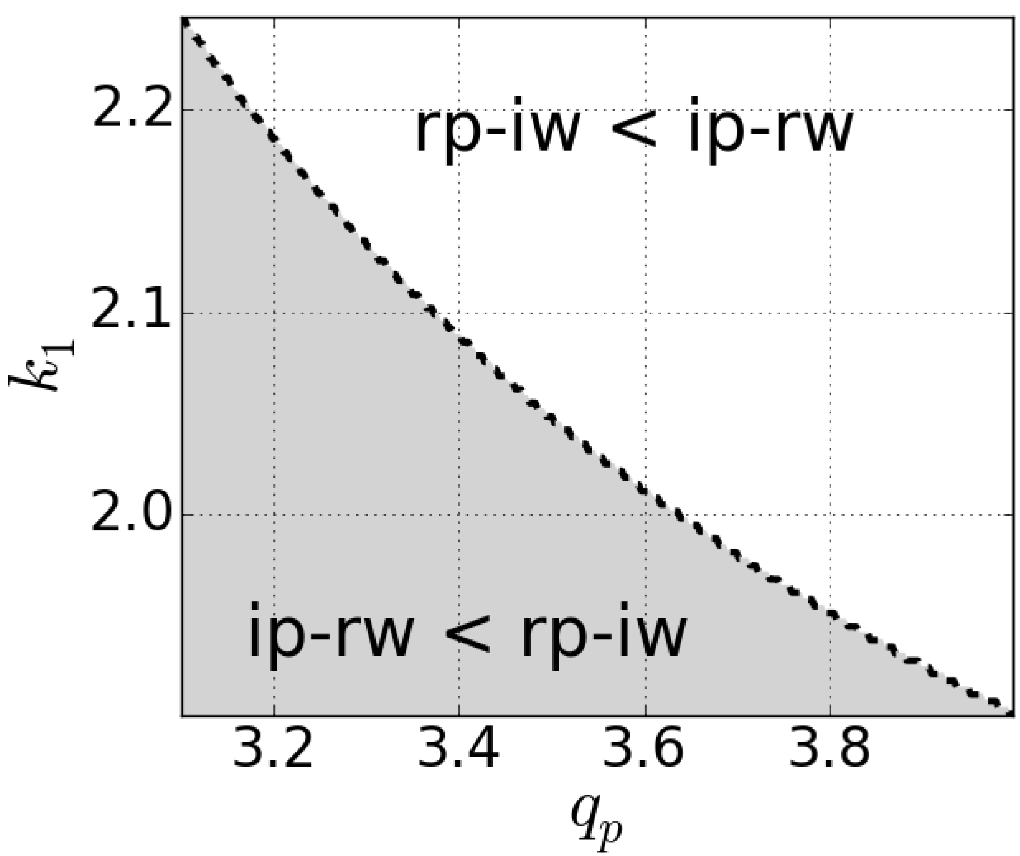

OUTLINE

Review the simple reduced MHD model with

- differential flow between surfaces and/or a wall
- a resistive wall
- feedback control from external coils
- toroidal field line curvature in a cylindrical model
- trapped energetic ions

Brief Review: 2016 Sherwood Theory Conference presentations

J.M. Finn	Toroidal mode coupling model derivation Double tearing vs. Toroidal coupling via pressure
D.J. Rhodes	Beta ordering can change due to qmin or toroidal curvature, coupling Shaping effects important
D.P. Brennan	Toroidal coupling model explanation of 2/1 onset and rotation effect
M.R. Halfmoon	Energetic particle effects on resistive and ideal MHD modes explains effect of core shear
A.J. Cole	Locking to the backward propogating wave finite frequency modes drive flow at surface

Experimental Case With Low Beta 2/1 Tearing Mode on DIII-D

Current is ramped inductively for L-Mode discharge. Moderate sawteeth are observed (not shown). 2/1 Tearing mode becomes unstable and grows to lock and terminate the discharge.

Kinetic reconstructions taken before and after onset.

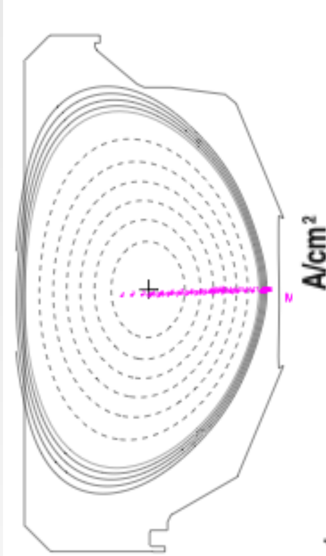

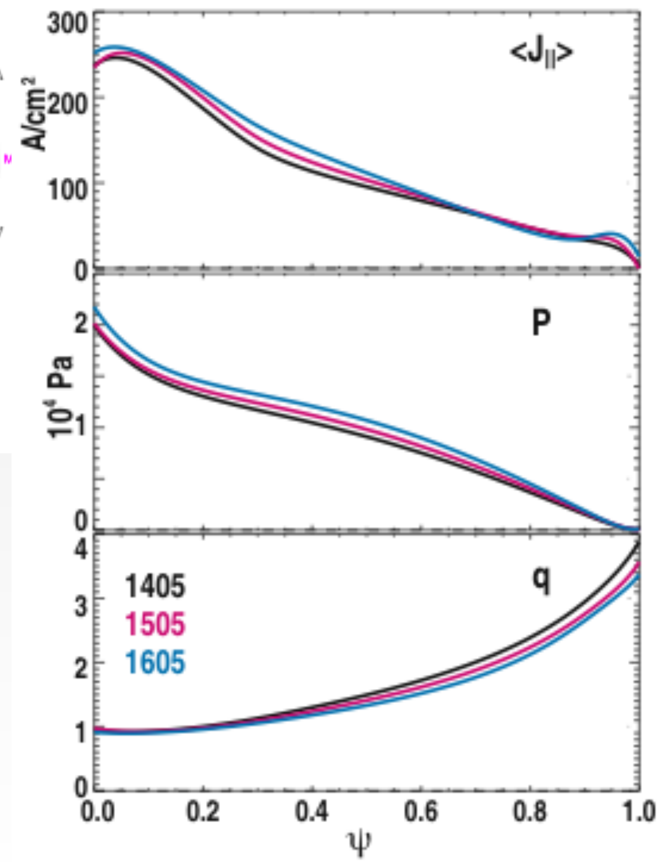

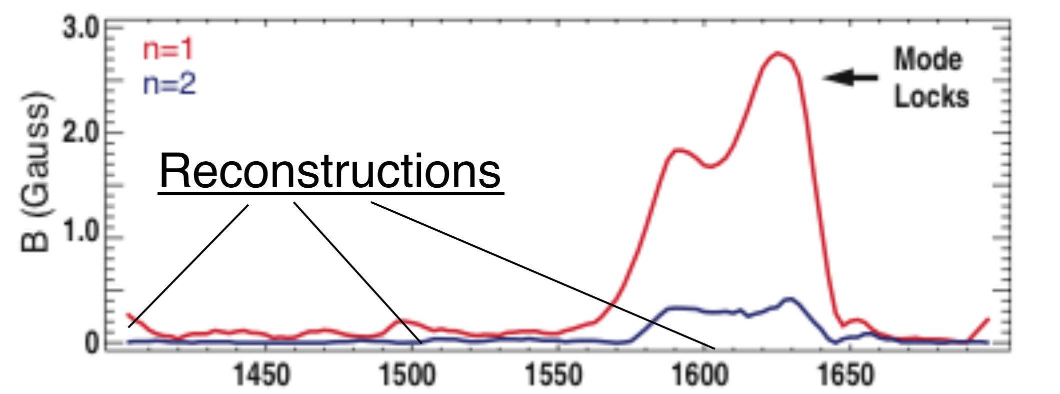

D.P. Brennan and L.E. Sugiyama, Physics of Plasmas 13, 052515 (2006)

M.S. Chu, R.J. La Haye, M.E. Austin et al., Phys. Plasmas **9**, 4584 (2002).

The Most Important Physics in the Onset of the 2/1 Mode are the Coupling to the 1/1 and the Effect of D_R

Summary:

Coupling to the q=1 is strongly stabilizing.

Finite D_R is also stabilizing.

The coupling to the q=3 surface is slightly destabilizing.

Reduced model helps understand Why is it damping to couple to the 1/1 mode?

Answer: Quadratic roots
More unstable mode driven (1/1), less unstable damped (2/1). This analysis isolated the 2/1 root.

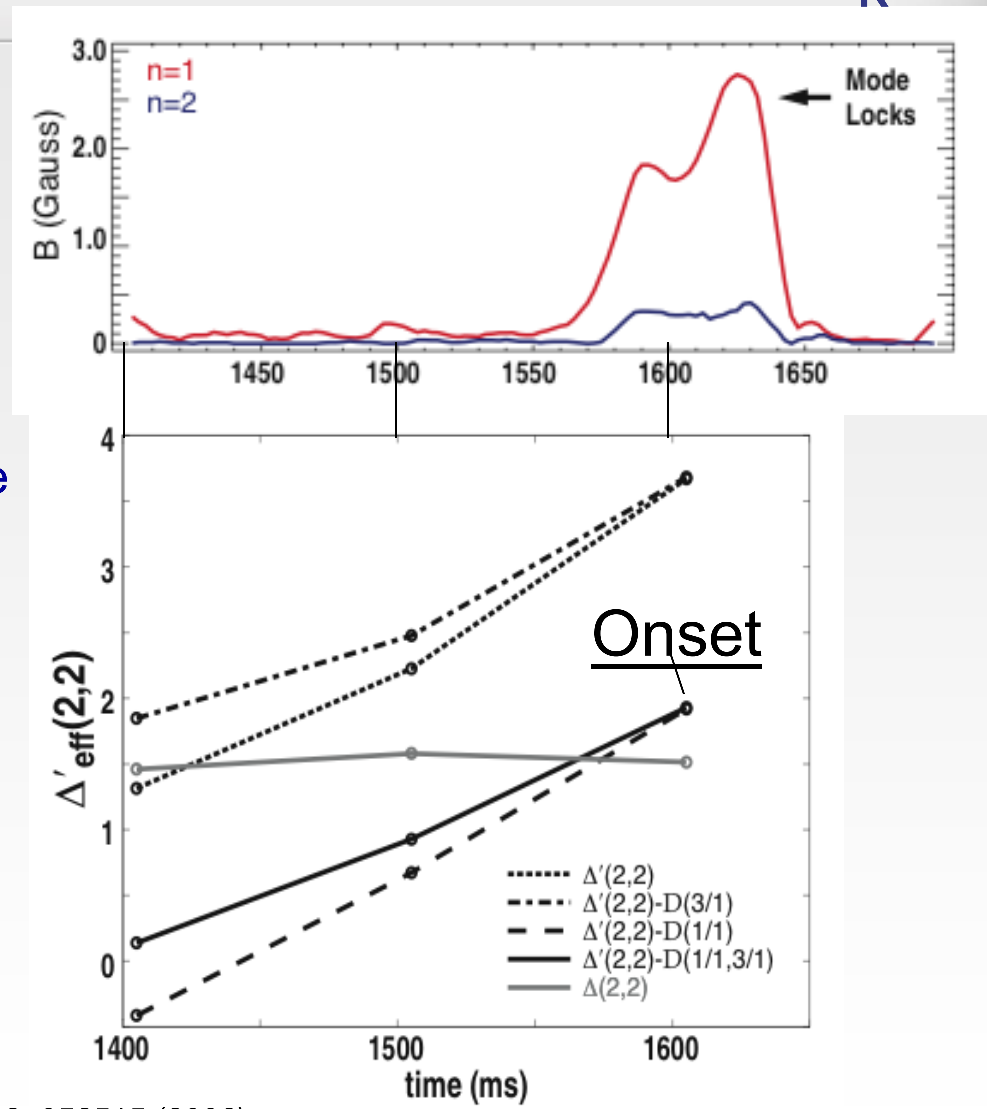

D.P. Brennan and L.E. Sugiyama, Physics of Plasmas 13, 052515 (2006)

Note: there is a disconnect between the purely cylindrical model and including toroidal curvature

Note that if $\kappa_0 \to -r/R_0^2 q^2$ (cylindrical poloidal only) then the pressure is destabilizing even when $\kappa_1 \to 0$

However, if $\kappa_0 \to -(1-q^2)r/R_0^2 q^2$ (includes toroidal curvature) then pressure is stabilizing for $q > 1$ even when $\kappa_1 \to 0$ and we lose the connection to the cylindrical.

Because $\kappa_1/\kappa_0 \approx a/R_0$ a convenient assumption is to use the cylindrical κ_0 though it's inconsistent with κ_1

$\kappa_0 = -r/R_0^2 q^2$
destabilizing

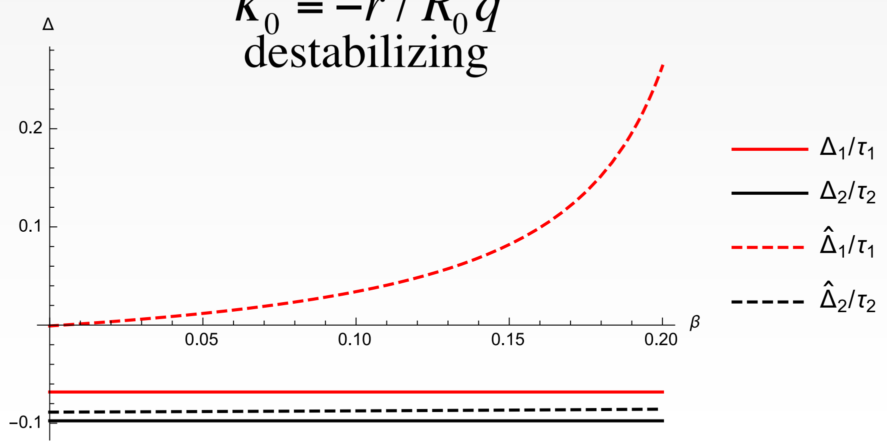

$\kappa_0 = -(1-q^2)r/R_0^2 q^2$
stabilizing

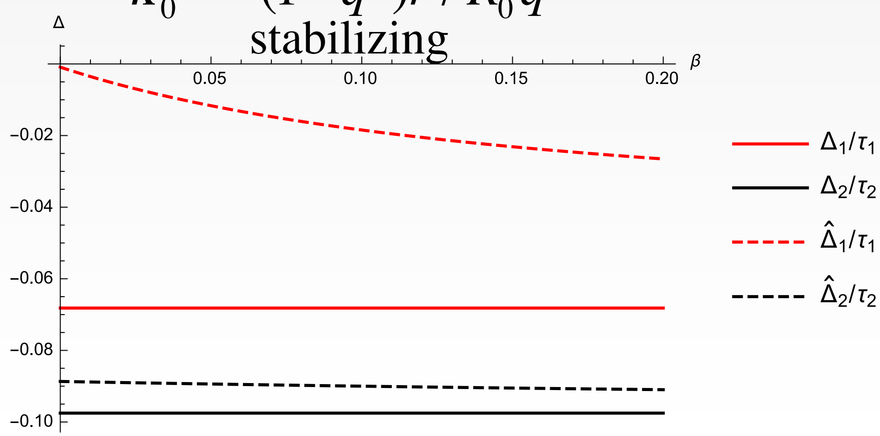

OUTLINE

Review the simple reduced MHD model with

- differential flow between surfaces and/or a wall
- a resistive wall
- feedback control from external coils
- toroidal field line curvature in a cylindrical model
- trapped energetic ions

Brief Review: 2016 Sherwood Theory Conference presentations

J.M. Finn	Toroidal mode coupling model derivation Double tearing vs. Toroidal coupling via pressure
D.J. Rhodes	Beta ordering can change due to qmin or toroidal curvature, coupling Shaping effects important
D.P. Brennan	Toroidal coupling model explanation of 2/1 onset and rotation effect
M.R. Halfmoon	Energetic particle effects on resistive and ideal MHD modes explains effect of core shear
A.J. Cole	Locking to the backward propogating wave finite frequency modes drive flow at surface

Typical Hybrid discharge: 3/2 tearing mode and hovering q_{min}>~1

Tokamak hybrid experiments commonly show an m/n=3/2 neoclassical tearing mode (NTM) onset during the β ramp up and flattop before the onset of an m/n=2/1 NTM.

3/2 mode onsets when q=1.5 comes into existence, and continues in nonlinear state.

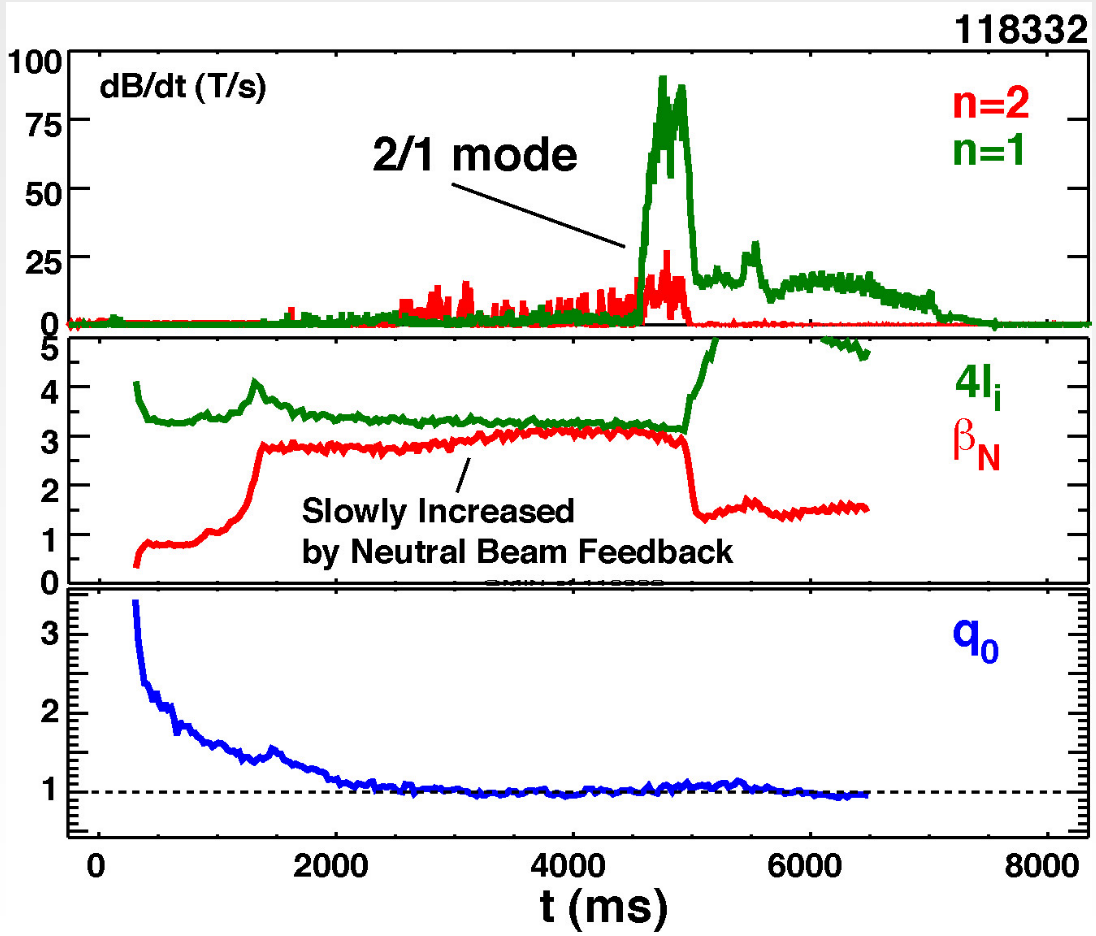

DIII-D NATIONAL FUSION FACILITY SAN DIEGO

Equilibrium reconstruction has q_{min}≥1 : Stability differs from high q_{min} by near axis response

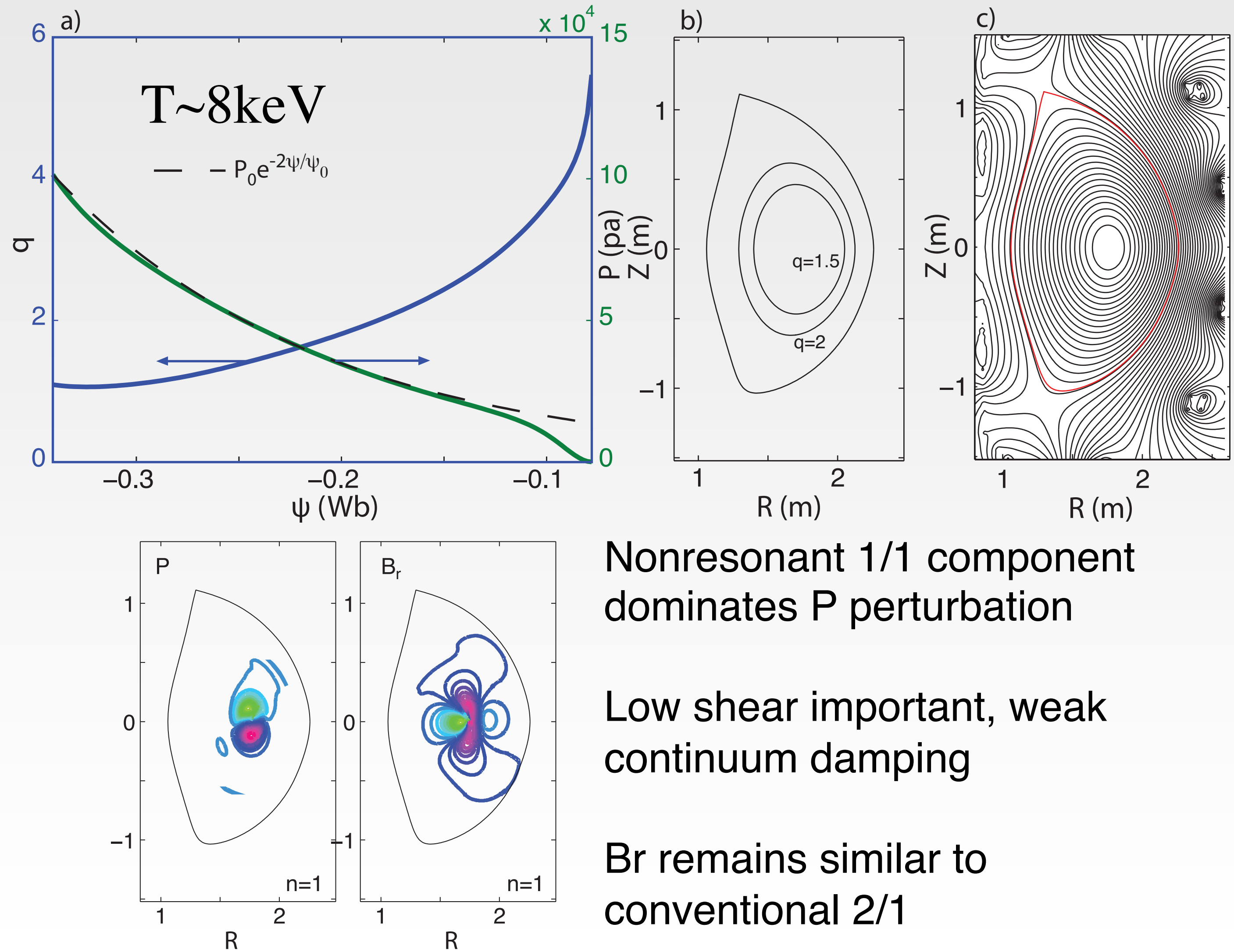

Nonresonant 1/1 component dominates P perturbation

Low shear important, weak continuum damping

Br remains similar to conventional 2/1

Stability map of MHD only agrees with equilibrium reconstruction, but not increase in β_N

Experiment hovers just outside the n=1 unstable zone in this discharge.

However, increases in β_N of small amounts ~0.2 cause onset of the 2/1 mode.

Puzzle: why is the stability boundary not even in the right direction? Indicates stable region at higher β_N.

Are particles responsible?

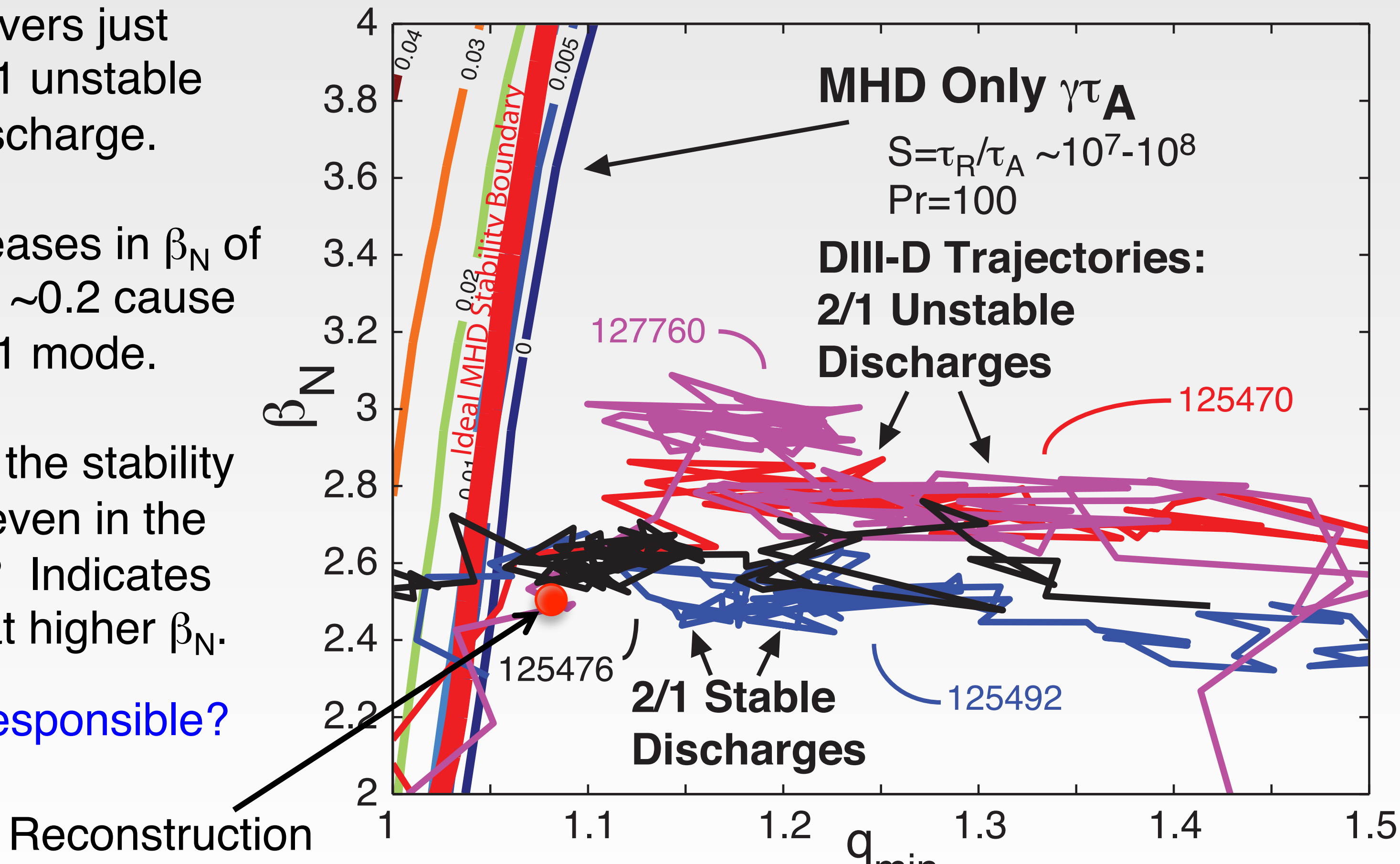

For more on experiment: La Haye et al. Nucl. Fusion 2010

Stability analyses: D.P. Brennan et al. Nucl. Fusion 2012

Introduce δf kinetic – MHD Analysis to Determine Effects of Energetic Ions

The slowing down distribution function is used

Constant C matches the equilibrium pressure profile

$$f = \frac{P_0 \exp(P_\zeta / \psi_n)}{\varepsilon^{3/2} + \varepsilon_c^{3/2}}, \quad P_\zeta \propto \psi, \quad \psi_n = C\psi_0$$

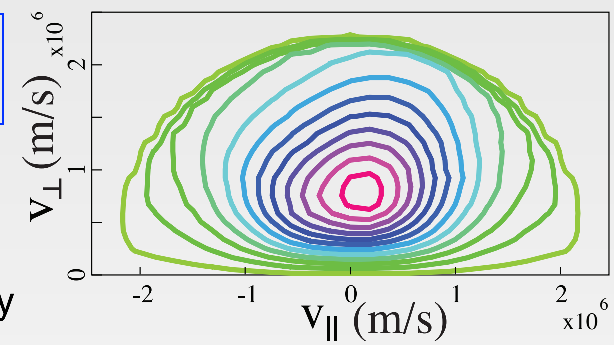

ε_c models the peak in f while a max initial v models the birth energy

The linearized evolution equation for δf becomes

$$\delta\dot{f} = f_0 \{ \frac{mg}{e\psi_n B^3} [(v_{||}^2 + \frac{v_\perp^2}{2}) \delta\mathbf{B} \cdot \nabla B - \mu_0 v_{||} \mathbf{J}_\perp \cdot \delta\mathbf{E}]$$

$$+ \frac{\delta\mathbf{v} \cdot (\nabla\psi_p - \rho_{||} \nabla g)}{\psi_n} + \frac{3}{2} \frac{e\varepsilon^{1/2}}{\varepsilon^{3/2} + \varepsilon_c^{3/2}} \mathbf{v}_D \cdot \delta\mathbf{E} \},$$

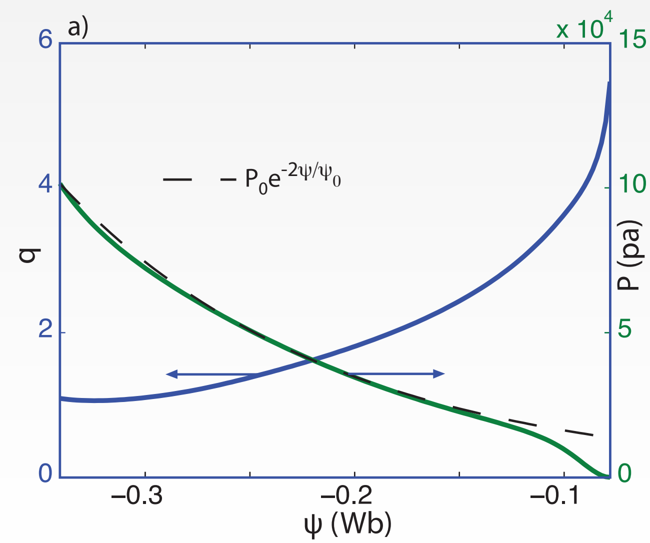

$$\mathbf{v}_D = \frac{mg}{eB^3} (v_{||}^2 + \frac{v_\perp^2}{2}) (\mathbf{B} \times \nabla B) + \frac{\mu_0 m v_{||}^2}{eB^2} \mathbf{J}_\perp,$$

where

$$\delta\mathbf{v} = \frac{\delta\mathbf{E} \times \mathbf{B}}{B^2} + \mathbf{v}_{||} \frac{\delta\mathbf{B}}{B}$$

Series of q_{min} at fixed pressure: Energetic particle driven modes up to high q_{min}

MHD unstable region: damped, low ω
MHD stable region: EP driven, $\omega >> \gamma$
ω lower than ω_{TAE}

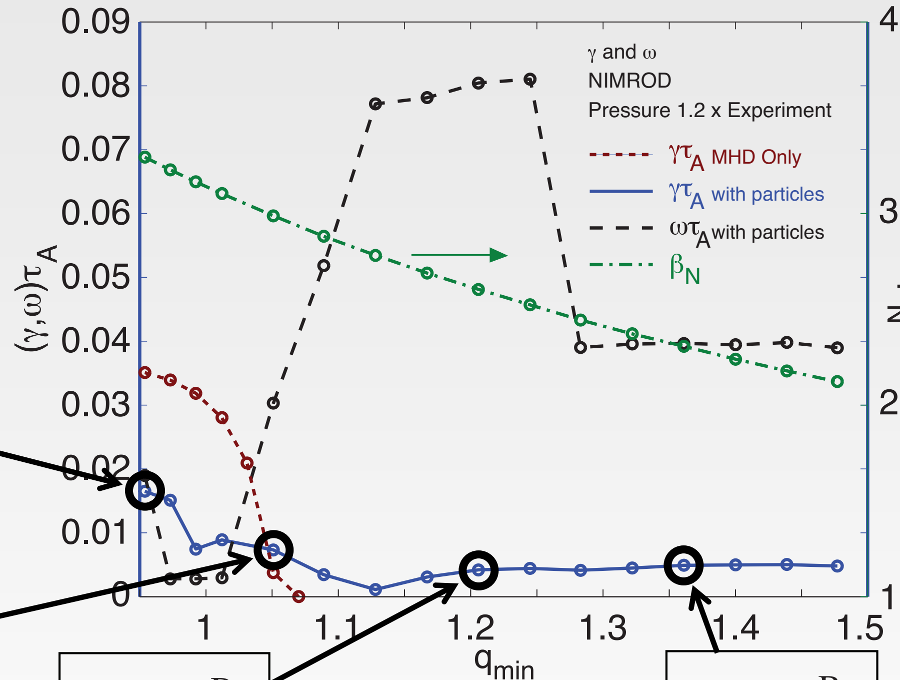

Low q_{min} has broad 1/1 structure moderate ω, damped γ

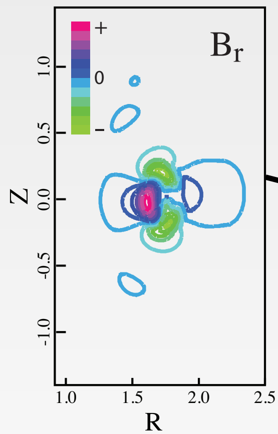

q_{min} >~1 has localized 1/1, increasing ω, decreasing γ, with q

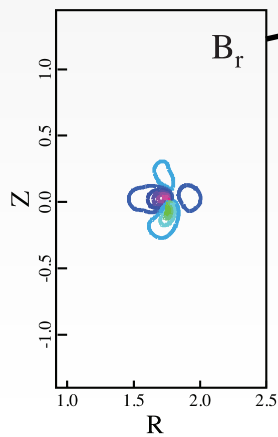

q_0>~1.2 has broader 1/1, high ω, driven γ

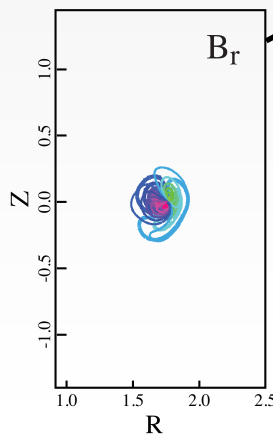

q_{min}=1.36 dominantly 2/1, moderate ω, driven γ

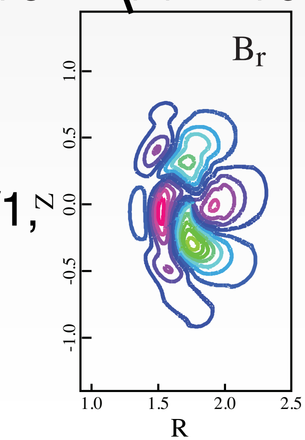

Particle interaction differs in core and outside of core, changes in resonant location important

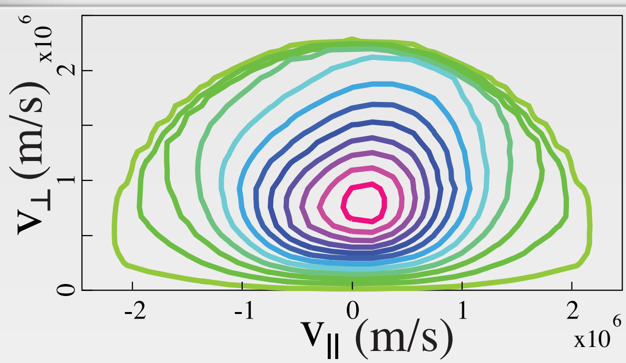

The total distribution at each point as a function of parallel and perpendicular velocity

$$\delta f(v_{\parallel}, v_{\perp})_{n=1} = \int_{r_1}^{r_2} \delta f(\mathbf{z}) d^3x \Big|_{n=1}$$

q_{min}=1.05
1/1 core localized

q_{min}=1.21
high frequency
energetic particle mode

q_{min}=1.36
broad 2/1 mode
frequency lower

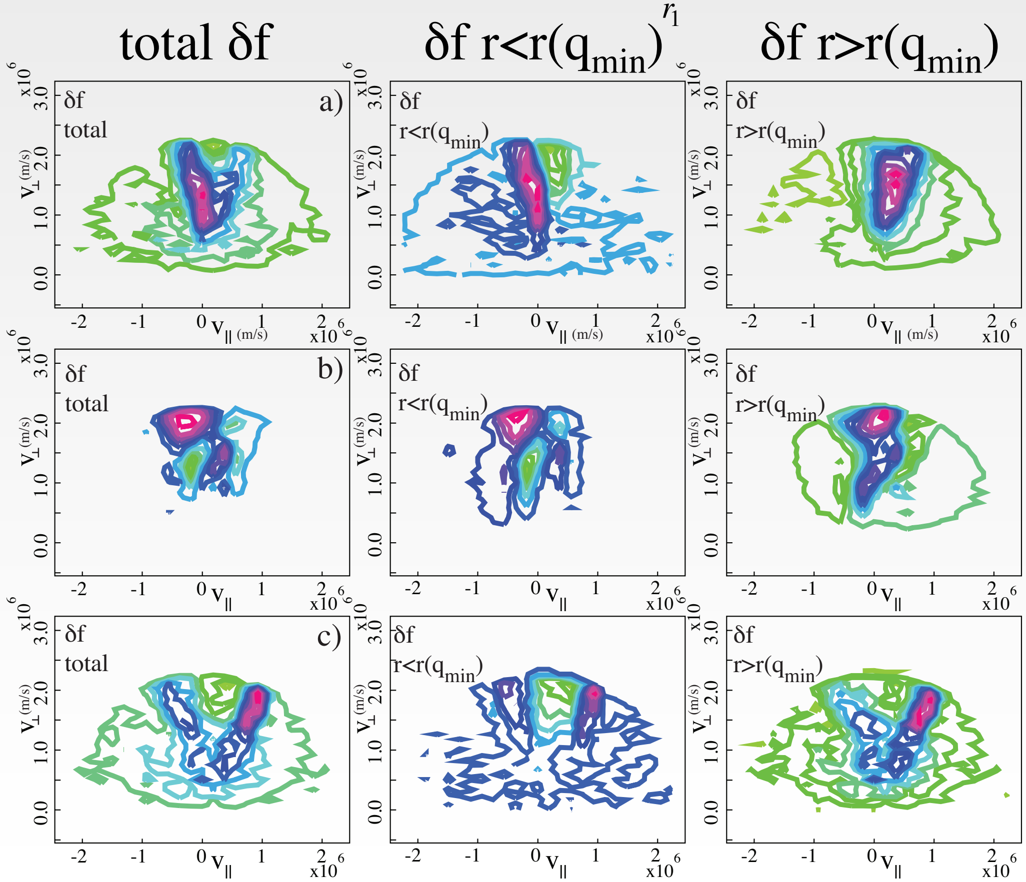

Mode frequency comparable to toroidal precession frequency of resonant particles

Precession frequency estimate

$$\omega_p \approx \frac{nqE_{eV}}{r_m R_0 B_0}$$

Power flow particles to mode

$$\frac{dU}{dt} = e\omega v_d \cdot (B \times \xi) e^{-i(\omega t - \omega_p t)}$$

is only steady state with frequency match -> mode structure changes cause frequency to change.

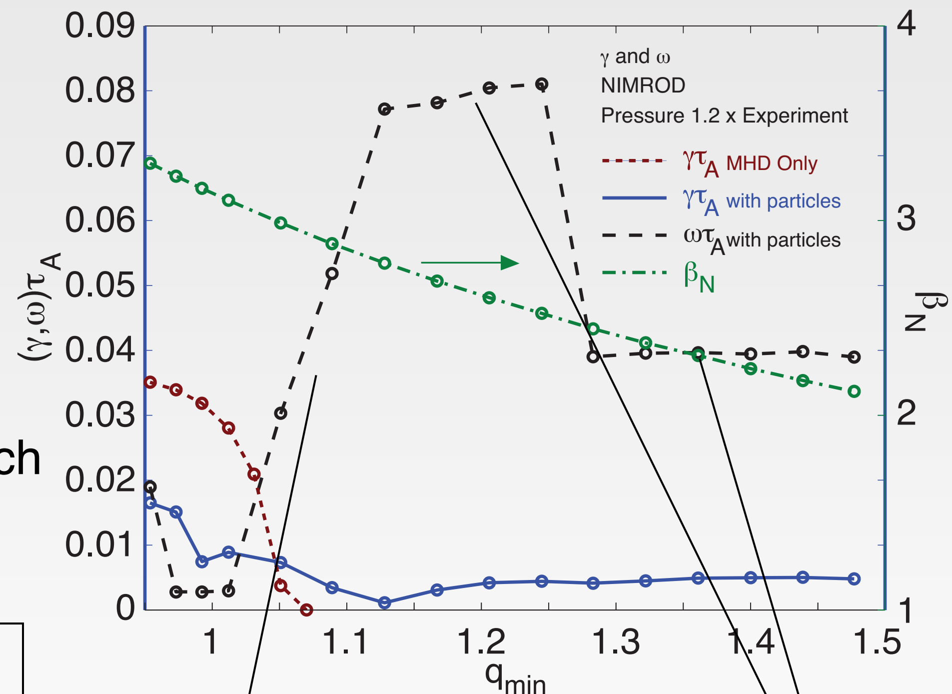

For higher q_{min} modes:

resonant q changes=>

ω changes=>

$q_{\min} \approx 1.2$	$q_{\min} \approx 1.4$
$E_{eV} \approx 30keV$	$E_{eV} \approx 30keV$
$B_0 \approx 2T$	$B_0 \approx 2.3T$
$r_m \approx 0.05m$	$r_m \approx 0.25m$
$q \approx 1$	$q = 2$
$\omega_p \tau_A \approx 0.09$	$\omega_p \tau_A \approx 0.04$

For low $q_{\min} \approx 1$ resonant energy increases with q. Fishbone mode.

$\omega \sim \sqrt{\beta q}$ fixed with q. BAE modes.

D.P. Brennan et al Nucl. Fusion (2012)

δf kinetic – MHD analysis strongly suggest why 2/1 mode onsets : destabilized by energetic particles

Destabilization well into high q_{min} regime
Experimental trajectory in a low growth rate region
Gradient in increasing β_N direction, mode destabilized
Resistive instability significant at $\gamma\tau_A$~0.005

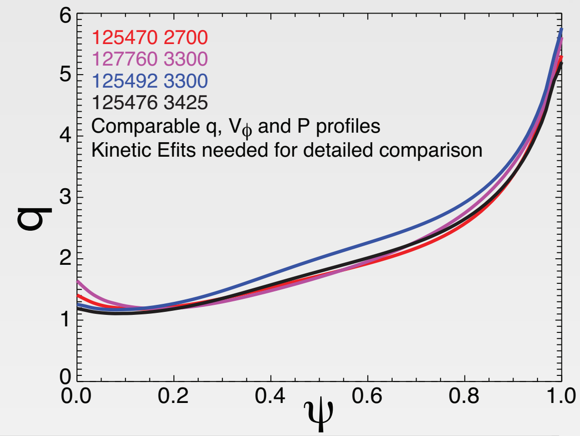

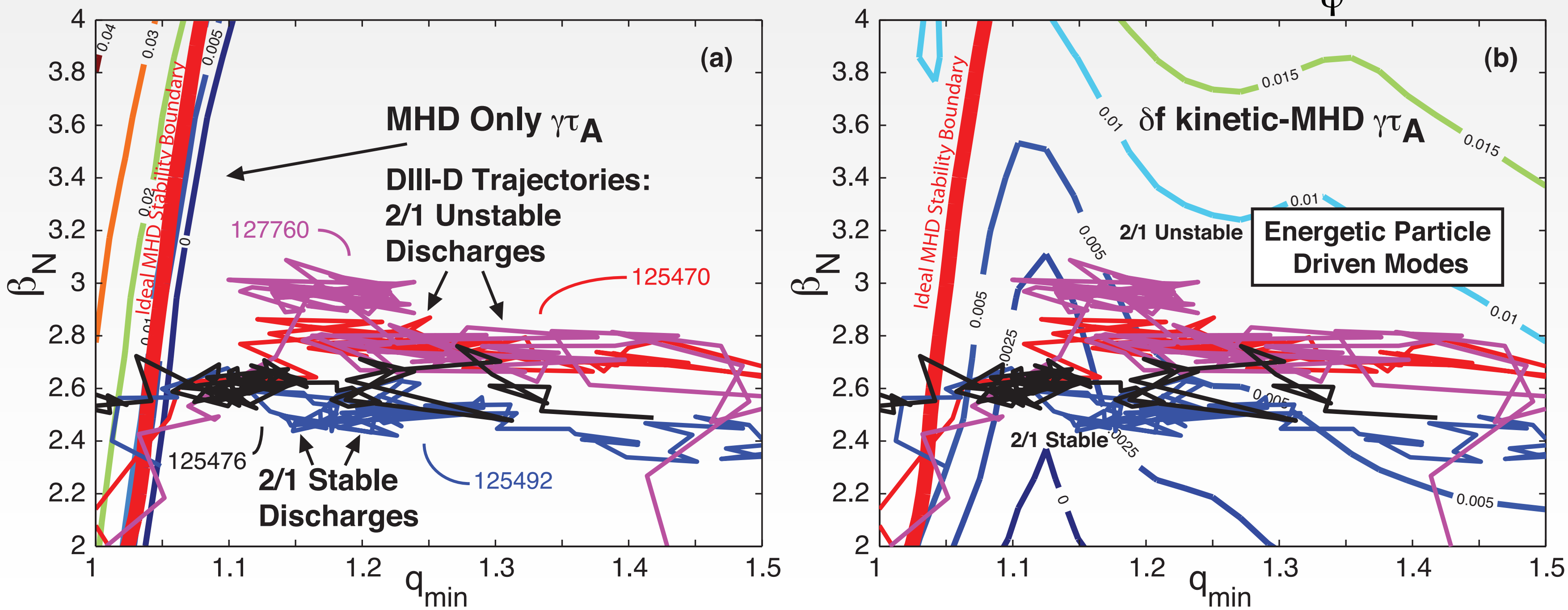

Puzzle: Slowing Down Distribution of Energetic Ions found Damping 2/1 Tearing Mode

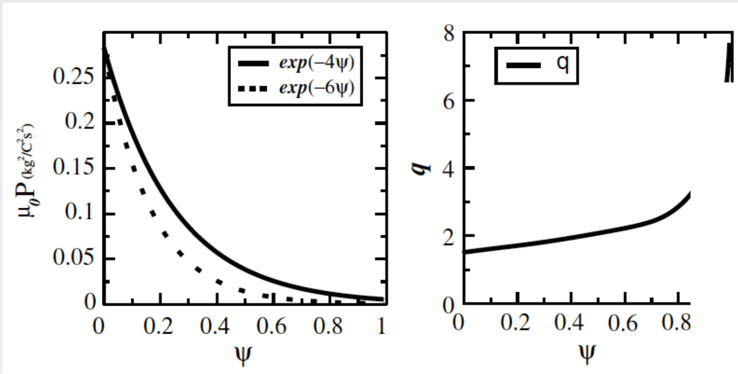

Robustly damping and stabilizing for equilibria with monotonic q.

Puzzle: Why is it damping here and destabilizing in the reversed shear case?
- > reduced model!

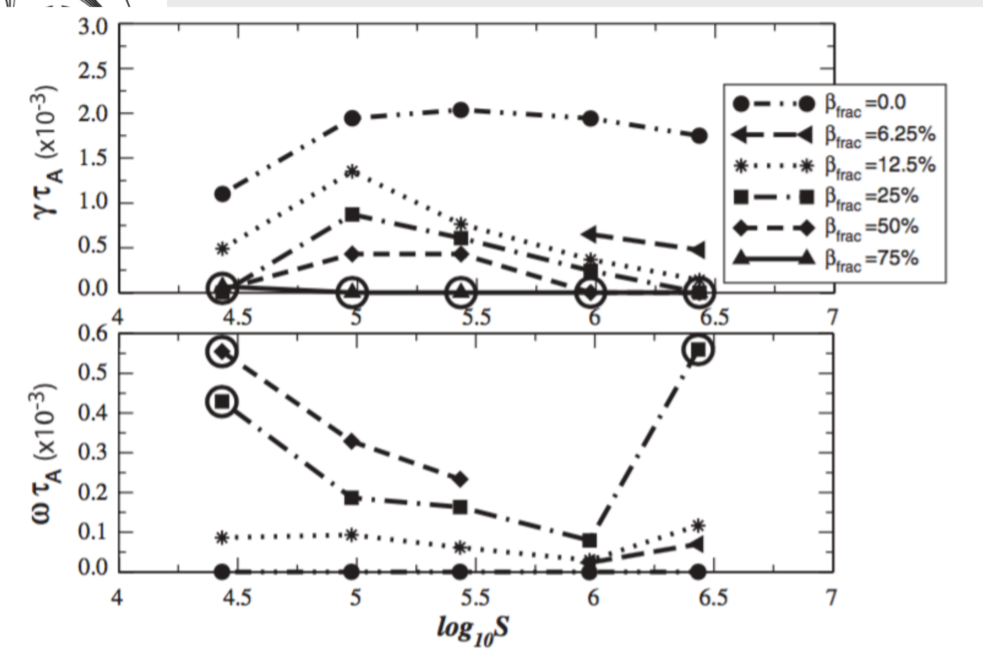

FIG. 4. The growth rates (upper panel) and the real frequency (lower panel) of the equilibrium $\beta_N/4l_i = 0.83$ for various β_{frac} as a function of S. Note that due to the adjustment of β_0, the equilibrium $\beta_N/4l_i$ does not change for various β_{frac}.

R. Takahashi, D.P. Brennan and C.C. Kim PRL 102, 135001 (2009)

Closely Related: Reduced Model of EP Effect on RWM Studied by Hu & Betti (PRL 2004)

- The energetic particle pressure contribution takes the form of a scalar modification to the perturbed pressure.

$$\tilde{p}_j^m = \frac{2^{5/2}\epsilon^{1/2}}{5\pi^{3/2}} \int_0^\infty d\hat{v}^5 e^{-\hat{v}^2} \int_0^1 du K(u) \Pi_j \sigma_m \sum_{\ell=-\infty}^{+\infty} \sigma_\ell Y_\ell^j$$

- In their work, this was then placed into a δW calculation to determine the stability of the resistive wall mode.

$$\delta W_K = \frac{1}{2} \sum_{j=i,e} \int d\mathbf{r} (\tilde{\boldsymbol{\xi}}_\perp^* \cdot \boldsymbol{\kappa}) \tilde{p}_j^K$$

$$\gamma \tau_w \simeq - \frac{\delta W_\infty + \delta W_K}{\delta W_b + \delta W_K}$$

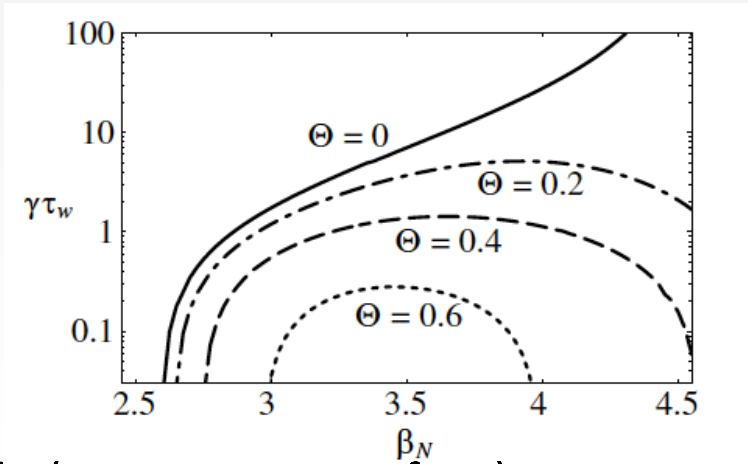

- Did not take into account the tearing mode (no resonant surface)

EP pressure integral models the resonant interaction of trapped particles with mode structure

- Where

$$\Pi_j = -N_j \frac{R}{2}\frac{dT_j}{dr}\frac{\hat{v}^2 - \frac{3}{2} + \frac{l_{T_j}}{l_{N_j}} + 2\frac{l_{T_j}}{R} w_E^j}{w_E^j + \hat{v}^2 H(u)}$$

$$\sigma_m = \int_0^{\pi/2} d\chi \frac{\cos[2(m-q)\arcsin(\sqrt{u}\sin\chi)]}{K(u)\sqrt{1-u\sin^2\chi}}$$

$$w_E^j = \frac{\omega_E}{\bar{\omega}_B^j},\ l_{T_j} = -T_j/(dT_j/dr),\ l_{N_j} = -N_j/(dN_j/dr)$$

$$\bar{\omega}_B^j = \frac{q v_{th}^2}{\Omega_c R r},\ \ H(u) = (2s+1) + \frac{E(u)}{K(u)} + 2s(u-1) - \frac{1}{2}$$

- u is the pitch angle variable, q is charge, Ω_c is the cyclotron frequency, and s is the magnetic shear.
- The step function characteristic of the equilibrium pressure enters the pressure moment through the temperature gradient in Π_j

Particle pressure moment reduced to scalar coefficient on equilibrium pressure, to enter into tearing model

Using the coupling to curvature, we can determine the poloidal harmonics of the energetic pressure perturbation

$$Y_l^j = \int_{-\pi}^{\pi} \frac{d\theta}{2\pi} e^{-il\theta} (\hat{v}^2 \tilde{\xi}_\perp \cdot \kappa + \frac{Z_j e}{T_j} \tilde{Z})$$

Due to the poloidal dependence of this reduces to:

$$Y_l^j = \hat{v}^2 [(\hat{\xi}_r \kappa_0 + \frac{Z_j e}{T_j} \tilde{Z}) \delta_{l=m} + \hat{\xi}_r \kappa_1 (\delta_{l=m+1} + \delta_{l=m-1})]$$

Thus, the particle pressure has the form:

$$\tilde{p}_j^m = \int_0^\infty d\hat{v}^5 f_0(\hat{v}) \int_0^1 du K(u) \Pi_j \sigma_m \hat{v}^2 \left\{ \left(\tilde{\xi}_r \kappa_0 + \frac{Z_j e}{T_j} \tilde{Z} \right) \sigma_m + \tilde{\xi}_r \kappa_1 (\sigma_{m-1} + \sigma_{m+1}) \right\}$$

Which reduces to $\tilde{p}_j^m = \lambda p_0$

Where λ contains all the information of the energetic particle response to the fields

Energetic Particle Contribution Enters Stability Equation at Pressure Step

We can solve the ideal outer region equations by solving for the jump conditions at the resonant surface, and pressure and current steps.

$$\left[\tilde{\psi}'\right]_{a_c} + \frac{m j_0}{a_c F(a_c)} \tilde{\psi}(a_c) = 0$$

$$\left[\tilde{\psi}'\right]_{a_s} = \gamma \tau_r \tilde{\psi}(a_s)$$

Particle Pressure

$$\left[\tilde{\psi}'\right]_{a_p} + \frac{2 m B_\theta(a_p) \beta_0}{a_p^2 F(a_p)} \left(\frac{m}{a_p F(a_p)} - \lambda \beta_{frac} \right) \tilde{\psi}(a_p) = 0$$

Pressure Enters in Δ' Calculation Indicating Damping and Stabilizing Effect on Resistive Mode

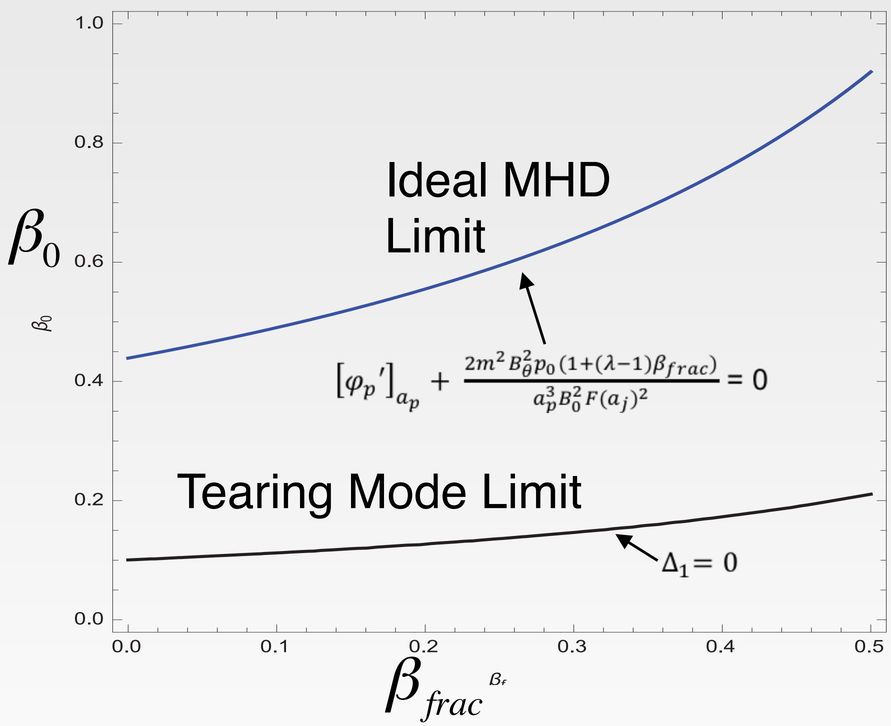

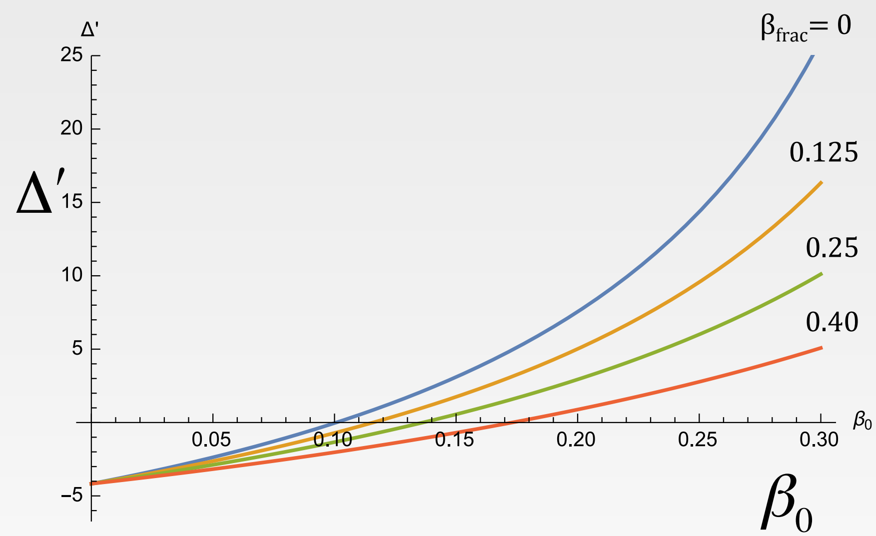

- One limitation of our model is that the precession frequency is a fixed value determined only by equilibrium quantities, and the mode itself is assumed to have no rotation.
- For this configuration, $\Delta' = [\varphi_s']_{a_s} + \frac{\varphi_s'(a_j+)\varphi_j'(a_s-)}{[\varphi_j']_{a_j} + \frac{j_0 m}{a_j F(a_j)}} + \frac{\varphi_s'(a_p-)\varphi_p'(a_s+)}{[\varphi_p']_{a_p} + \frac{2mB_\theta(a_p)\beta_0}{a_p^2 F(a_p)}\left(m\frac{1-\beta_{frac}}{a_p F(a_p)} - \lambda\beta_{frac}\right)}$

Consider an Equilibrium Configuration with a Second Pressure Step Inside the Plasma Column

- Second pressure step in zero shear region.
- Results with weak shear, reversed or not, from second current step indicate qualitative similar results
- Each pressure drive enters the stability equation separately due to the geometric configuration.
- At their separate step functions, local shear affects their contribution, -> stabilizing or destabilizing

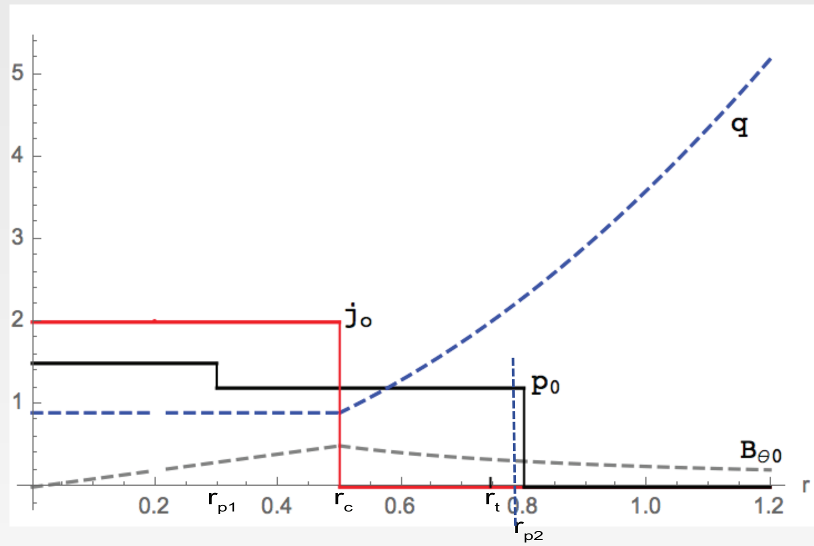

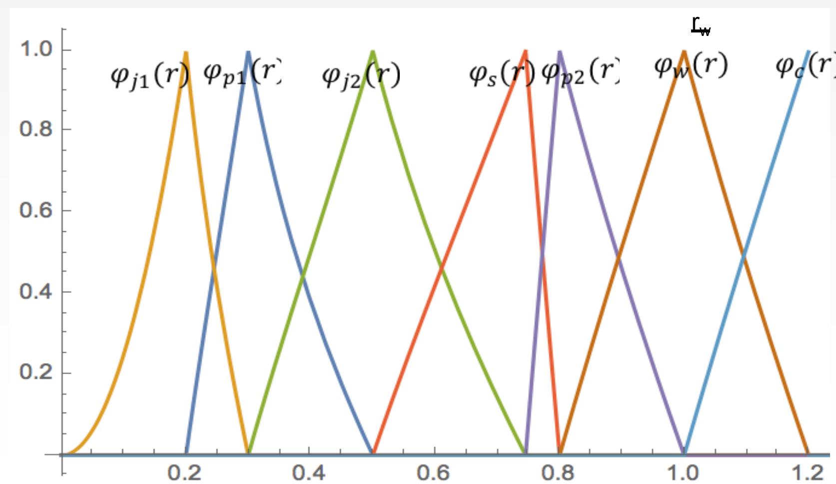

WHY? λ Plays a Role in Determining the Effect that Particles Have on Mode Stability -> changes sign

Jump across a pressure step

$$\left[\tilde{\psi}'\right]_{a_p} + \frac{2mB_\theta(a_p)\beta_0}{a_p^2 F(a_p)}\left(\frac{m}{a_p F(a_p)} - \lambda\beta_{frac}\right)\tilde{\psi}(a_p) = 0$$

For low shear, Π_j in the λ integral has a pole where $H(u) = 0$

$\omega_E = 0$ here

Integral switches sign, leads to destabilizing effect

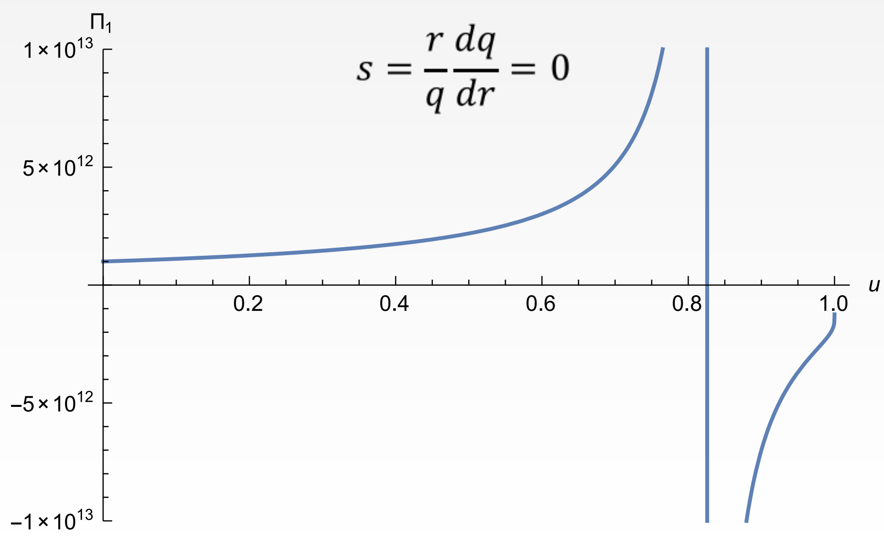

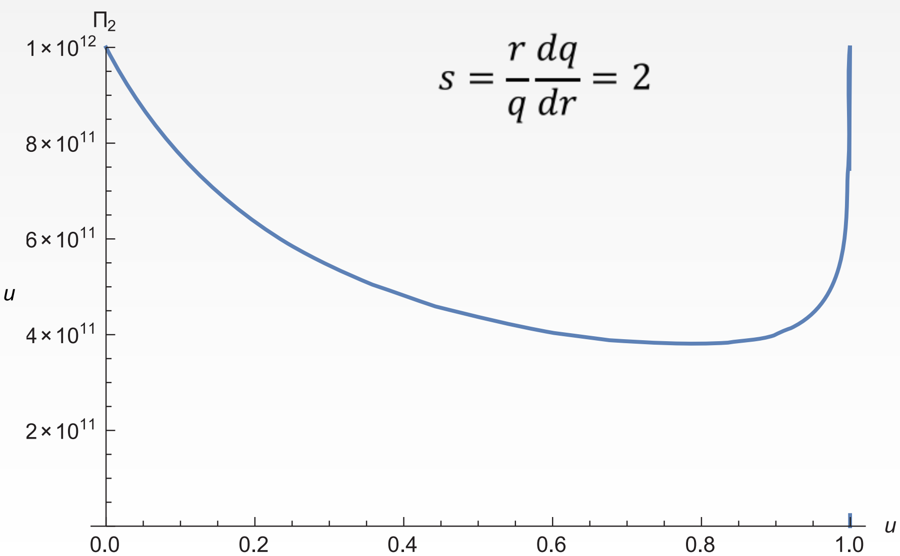

Δ’ Calculation Indicates a Destabilizing Effect for Equilibria with Internal Step

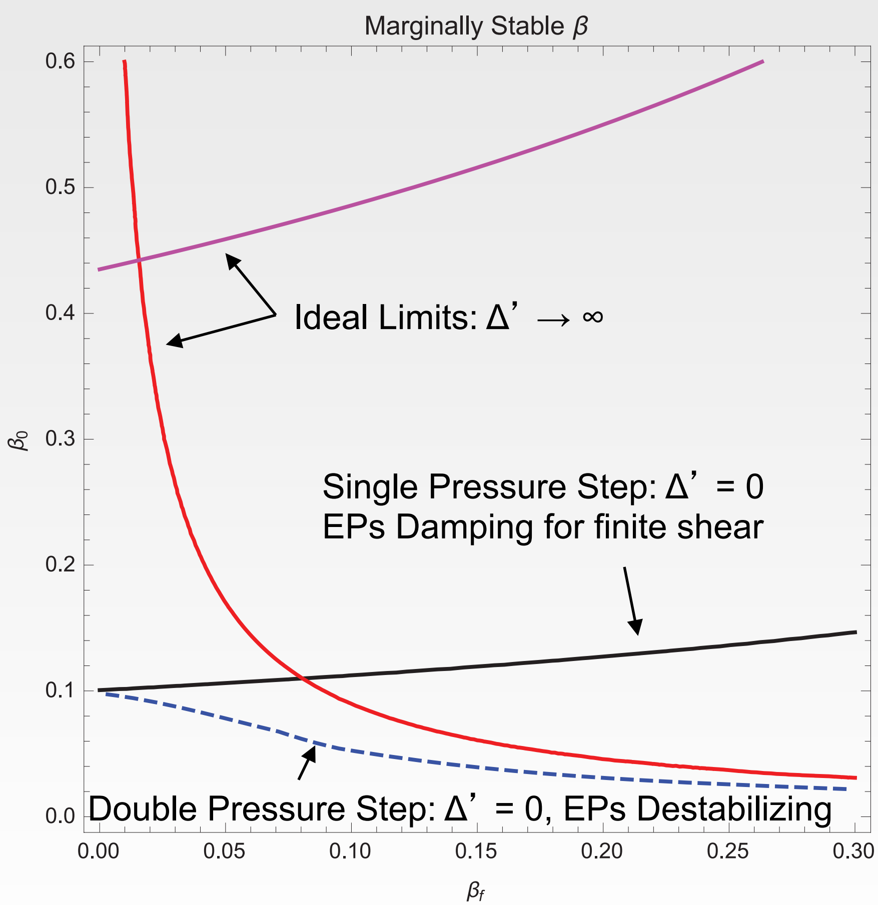

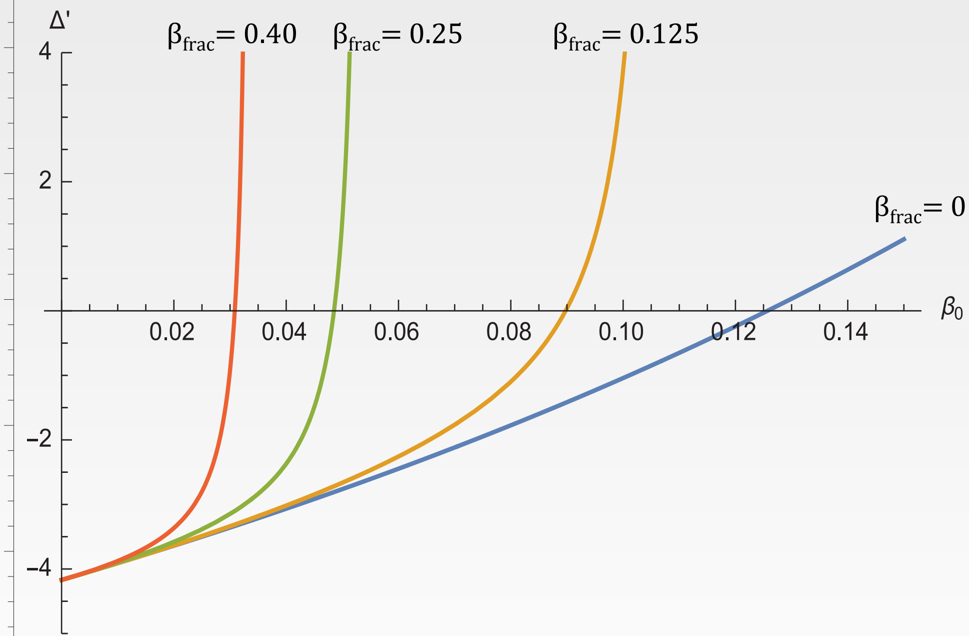

For the equilibrium configuration with an internal pressure step, particles contribute to the growth of the 2/1 tearing mode.

OUTLINE

Review the simple reduced MHD model with

- differential flow between surfaces and/or a wall
- a resistive wall
- feedback control from external coils
- toroidal field line curvature in a cylindrical model
- trapped energetic ions

Brief Review: 2016 Sherwood Theory Conference presentations

J.M. Finn	Toroidal mode coupling model derivation Double tearing vs. Toroidal coupling via pressure
D.J. Rhodes	Beta ordering can change due to qmin or toroidal curvature, coupling Shaping effects important
D.P. Brennan	Toroidal coupling model explanation of 2/1 onset and rotation effect
M.R. Halfmoon	Energetic particle effects on resistive and ideal MHD modes explains effect of core shear
A.J. Cole	Locking to the backward propogating wave finite frequency modes drive flow at surface

Review of spontaneous and driven tearing modes

Spontaneous modes

- TM are 'slow' growing: obey marginally stable (no inertia or viscosity) ideal MHD everywhere except near boundary layer at $k \cdot B_0 = 0$
- Dispersion relation from asymptotic matching logarithmic derivative in flux function across tearing layer

$$\Delta' = \Delta(\gamma - i\omega_r)$$

EF problem: driven response in stable plasma

- Consider static single harmonic (k) 3D field resonant on single surface; Replace $\gamma - i\omega_r \rightarrow ikV$
- EF induces net electromagnetic (Maxwell) force only on resonant surface

$$F_m \propto -|\tilde{\psi}_t|^2 \,\mathrm{Im}\,[\Delta(ikV)] \;\ldots\; \tilde{\psi}_t \propto \frac{\tilde{\psi}_w}{\Delta' - \Delta(ikV)},$$

with $\tilde{\psi}_w$ the error field strength at vessel wall, etc

- Model of EF locking: anomal. $\mu_\perp$ resists F_m: $F_m + F_\mu = 0 \rightarrow$ leads to bifurcation, hysteresis

RI-GGJ: a familiar regime with finite frequency modes

$$L_r \Delta' = 2.12 \left[(\gamma\tau - i\tau\omega_r)^{5/4} - \frac{\pi D}{4(\gamma\tau - i\tau\omega_r)^{1/4}} \right] \; \ldots \; D \sim -p'(1-q^2) < 0$$

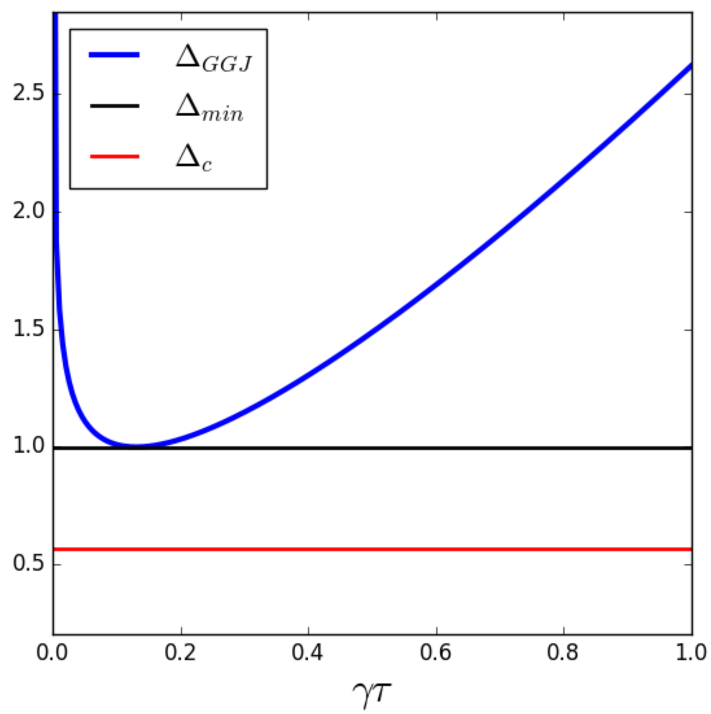

$\Delta(\gamma\tau)$ vs. $\gamma\tau$

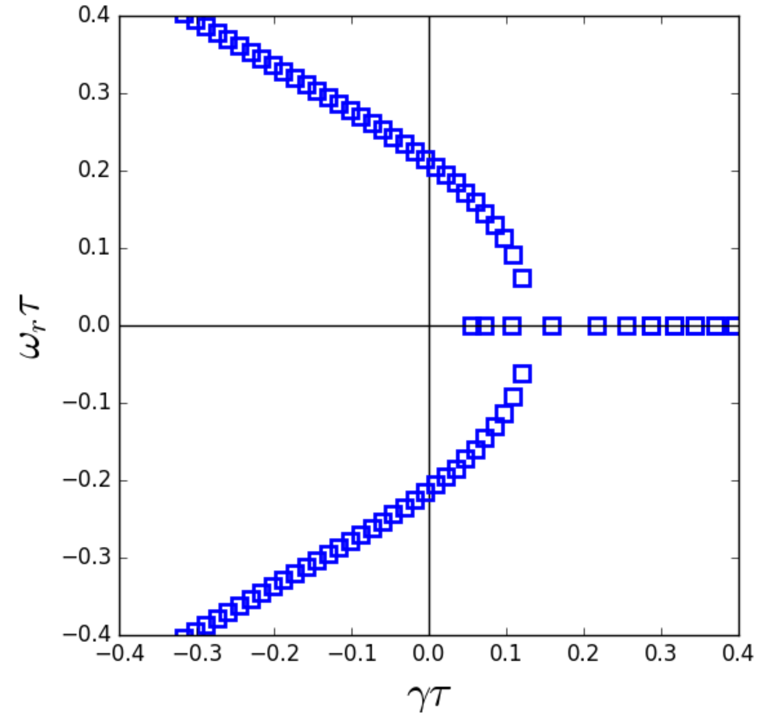

Locus of roots for RI with fixed $D < 0$, varying Δ'

complex roots if $L_r\Delta' < \Delta_{min}$,

stabilized if $L_r\Delta' < \Delta_c$

$L_r \propto S^{-1/3}$ and $\tau \sim S^{1/3}$

Driven EF problem sweeps along imaginary axis, distance to poles in $\tilde{\psi}_t$ influences force amplitude

$$F_m \propto -\left|\tilde{\psi}_t\right|^2 \mathrm{Im}\left[\Delta(ikV)\right] \;\ldots\; \tilde{\psi}_t \propto \frac{\tilde{\psi}_w}{\Delta' - \Delta(ikV)}$$

- Typical of inhomogeneous solutions: dispersion relation in denominator
- Zeros of $\mathrm{Im}\left[\Delta(ikV)\right]$ at locus crossings (and $V = 0$)
- Plasma conditions determine appropriate Δ, layer regime
- Note: two-fluid regimes lack symmetry in $\pm\omega_r$, $\omega_{*i,e}$

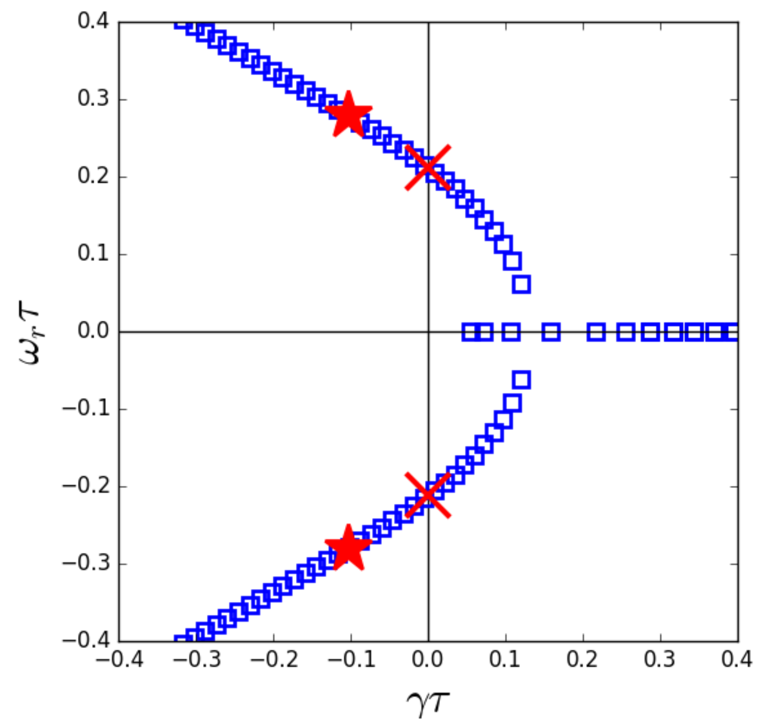

EF Maxwell force zero and largest magnetic flux observed when surface flows at rate $V \sim \omega_r / k$

$$F_m \propto -|\tilde{\psi}_t|^2 \,\mathrm{Im}\,[\Delta(ikV)] \sim -\frac{\Delta_i(ikV\tau)}{(L_r\Delta' - \Delta_r(ikV\tau))^2 + \Delta_i(ikV\tau)^2}$$

Numerator = 0 where $\Delta_i = 0$; denominator minimum nearby, both $\omega_r \approx kV$

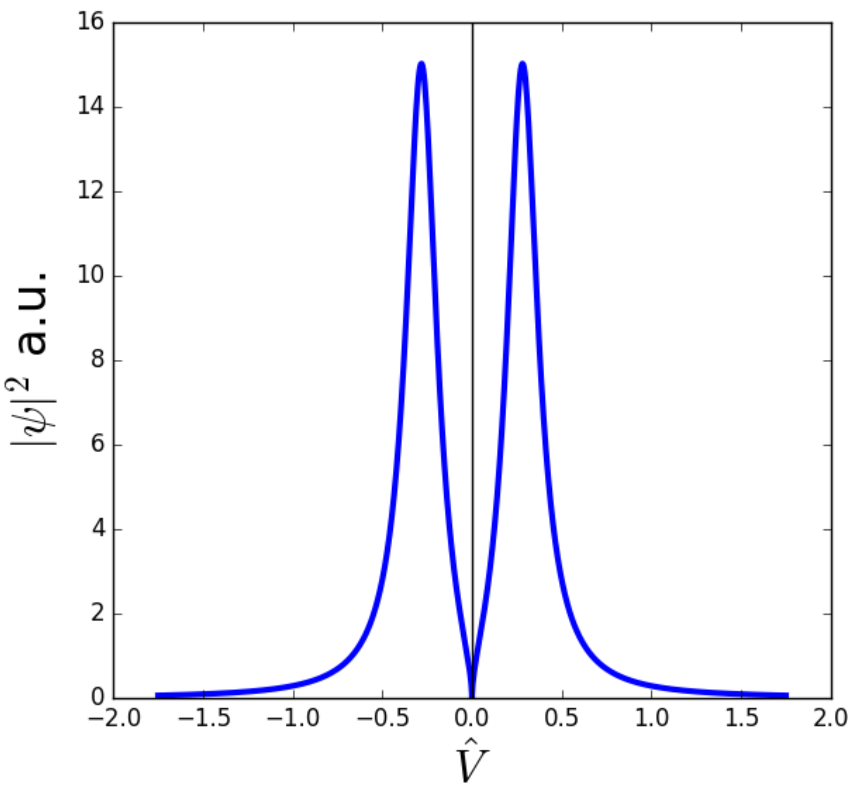

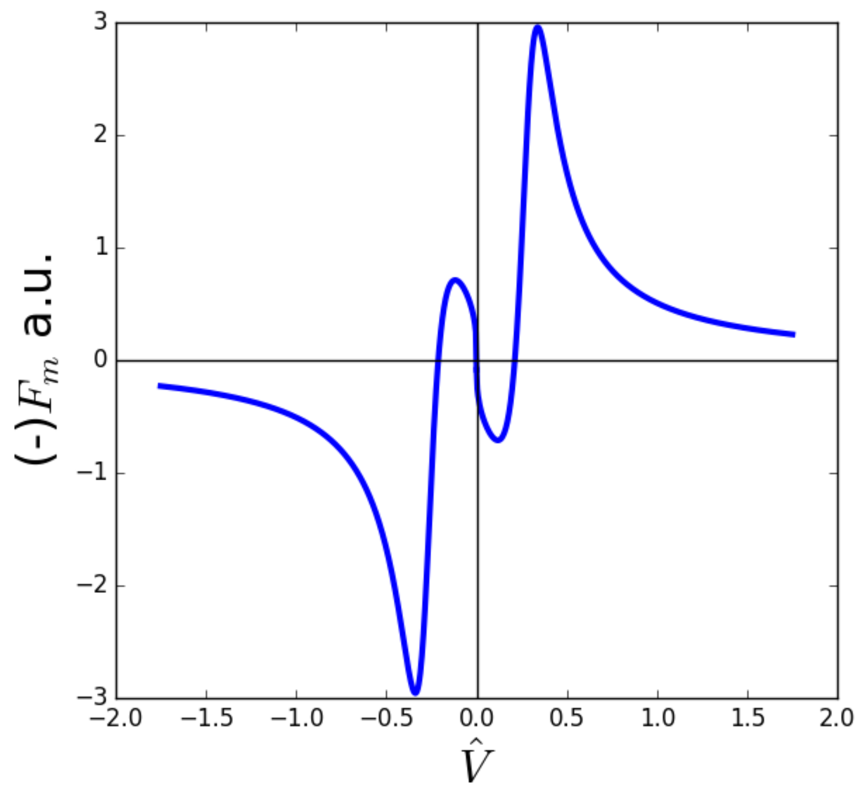

- New: pronounced peaks in $|\psi(r_t)|^2$ off axis, $L_r\Delta' = 0.25$
- New: zero of F_m at finite value of $\hat{V}$!

Main result: Fields are locked to static error field, plasma flow locked to finite value $V \gtrsim \omega_r/k$

Steady state force balance $F_m + F_\mu = 0$, with $F_\mu \propto \mu(V_0 - V)$ viscous force across layer and

$$F_m \propto -\frac{\Delta_i(ikV\tau)}{(L_r\Delta' - \Delta_r(ikV\tau))^2 + \Delta_i(ikV\tau)^2}$$

Different ways to induce bifurcation. Decreasing μ equiv. to increasing $\tilde{\psi}_t$

- Large μ: 3 roots (2 stable, 1 unstable)
- Intermediate μ intersects at $V \gtrsim \omega_r/k$.
- **Driven B field** locked to static EF
- **Flow** locked to $V \gtrsim \omega_r/k$; not $V \gtrsim 0$. Asymptote $V \not\to 0$.
- For very small μ two other states are possible.

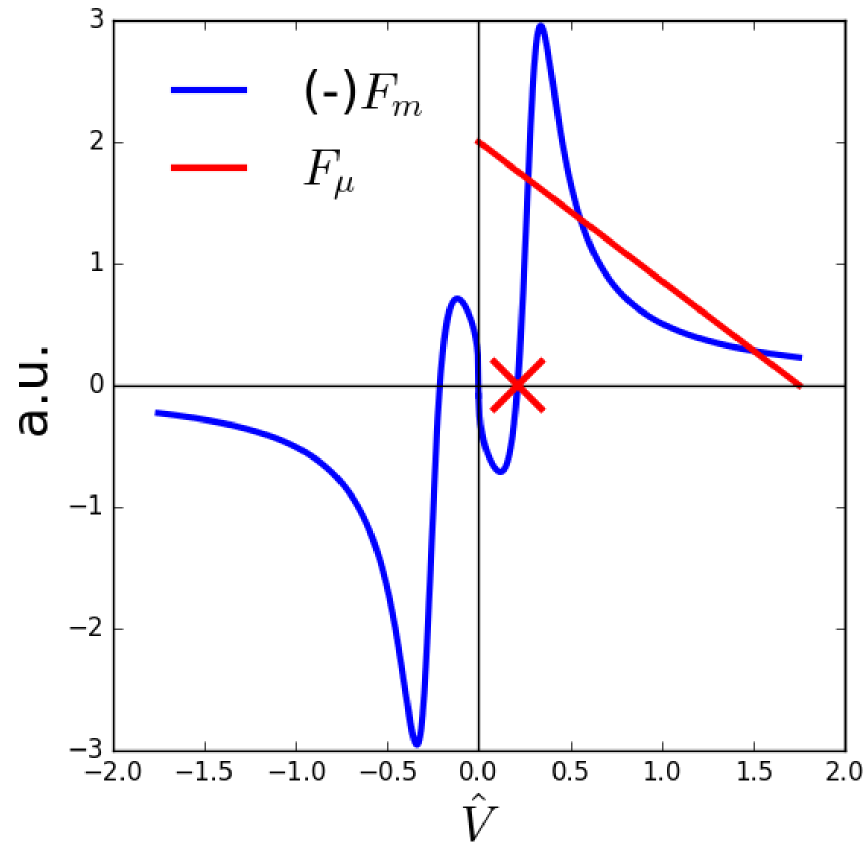

EF force balance exhibits bifurcation to a high reconnected flux, low flow “locked” state

- Two different aspects of the same bifurcation behavior

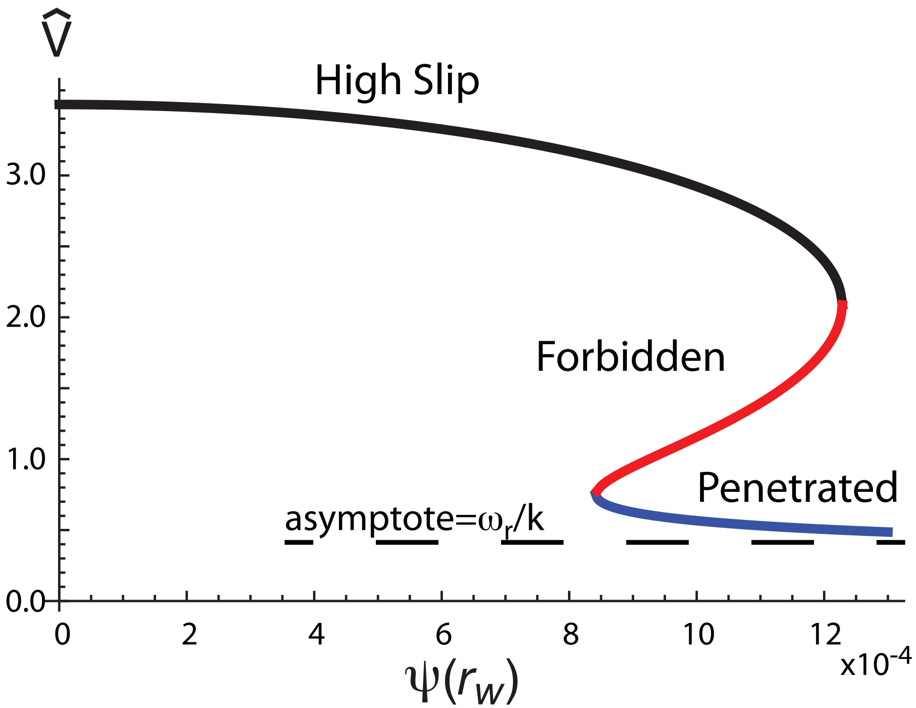

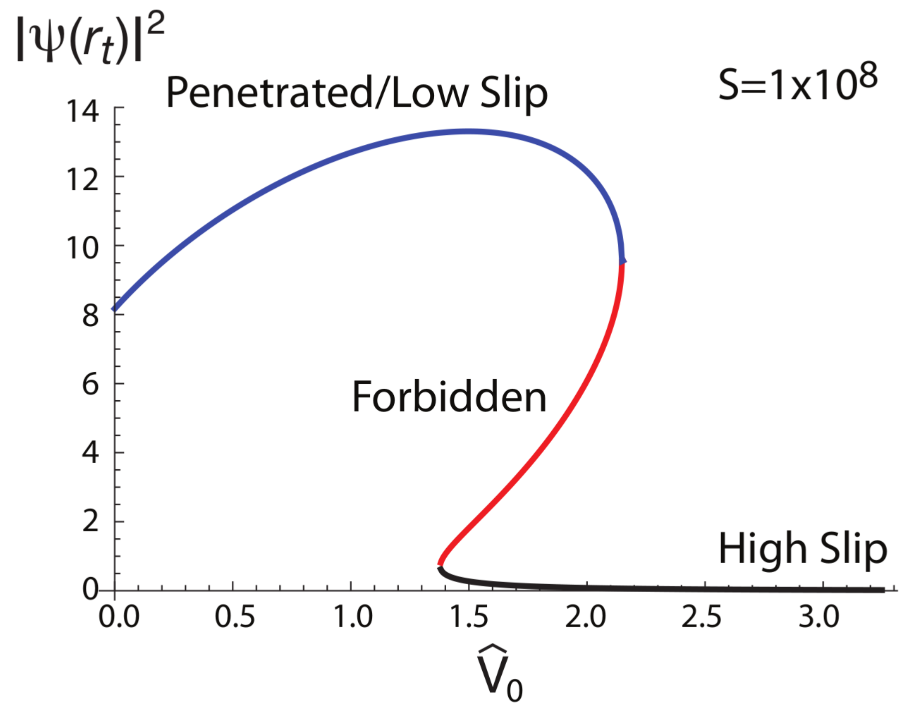

- Fixed initial velocity $\hat{V}_0$, increasing $\tilde{\psi}(r_w)$
- Fixed $\tilde{\psi}(r_w)$, decreasing $\hat{V}_0$

SUMMARY

Analyses of computational and experimental puzzles involving extended MHD instabilities with reduced modeling -> Combination leading to new discoveries

Recipe for our approach to reduced MHD step-function modeling

- differential flow between surfaces and/or a wall
- a resistive wall
- feedback control from external coils
- toroidal field line curvature in a cylindrical model
- trapped energetic ions

J.M. Finn	Toroidal mode coupling model derivation Double tearing vs. Toroidal coupling via pressure
D.J. Rhodes	Beta ordering can change due to qmin or toroidal curvature, coupling Shaping effects important
D.P. Brennan	Toroidal coupling model explanation of 2/1 onset and rotation effect
M.R. Halfmoon	Energetic particle effects on resistive and ideal MHD modes explains effect of core shear
A.J. Cole	Locking to the backward propogating wave finite frequency modes drive flow at surface

Ideas for Future Work

Do the different β orderings relate to experimental observations of tearing vs. RWM onset? $\beta_{rp,iw}<\beta_{ip,rw}$ vs. $\beta_{rp,iw}<\beta_{ip,rw}$

Analysis of nonlinear simulations indicating finite frequency locking and driven flow

Quasilinear mode locking between surfaces of different m

Rutherford modeling (ala Fitzpatrick 15)

Energetic particle effects on Resistive Plasma – Resistive Wall mode with flow

Coupling to the non-resonant 1/1 mode